BOEING MILITARY AIRPLANE SYSTEMS DIVISION

JANAIR

JOINT ARMY-NAVY AIRCRAFT INSTRUMENTATION RESEARCH

JANAIR REPORT 690104
ONR Contract
N00014-68-C-0289
NR 213-065

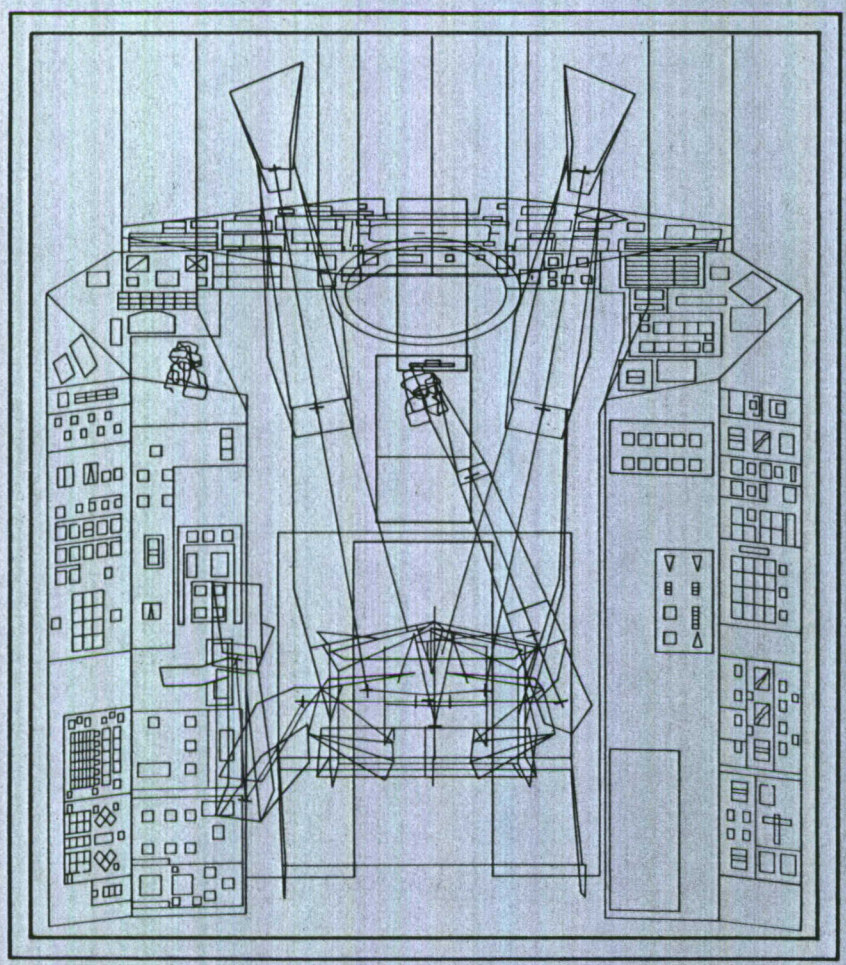

Supervised by P.H. Stern

Approved by V.G. Vaden

Jointly Sponsored By:

- Office of Naval Research
- Naval Air Systems Command
- U.S. Army Electronics Command

COCKPIT GEOMETRY EVALUATION

PHASE I FINAL REPORT
VOLUME IV–MATHEMATICAL MODEL

JANUARY 1969

D162-10128-1

COCKPIT GEOMETRY EVALUATION

PHASE I

FINAL REPORT

VOLUME IV–MATHEMATICAL MODEL

Prepared for
Joint Army-Navy Aircraft Instrumentation Research Program

Office of Naval Research,
Department of The Navy
under
Contract N00014-68-C-0289
NR 213-065

Programmer/Analyst, Computing Dept M.J. Healy
M.J. Healy

Coordinator, Computing Dept R. Katz
R. Katz

Group Supervisor, Computing Dept Robert R. Vaughn
R.R. Vaughn

Unit Chief, Computing Dept John S. Ryter
J.S. Ryter

Project Director Wayne E. Springer
W.E. Springer

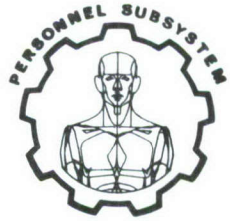

FOREWORD

This report presents work which was performed under the Joint Army Navy Aircraft Instrumentation Research (JANAIR) Program, a research and exploratory development program directed by the United States Navy, Office of Naval Research. Special guidance is provided to the program for the Army Electronics Command, the Naval Air Systems Command, and the Office of Naval Research through an organization known as the JANAIR Working Group. The Working Group is currently composed of representatives from the following Offices:

U. S. Navy, Office of Naval Research
Aeronautics, Code 461, Washington, D. C.
- Aircraft Instrumentation and Control Program Area

U. S. Navy, Naval Air Systems Command
Washington, D. C.
- Avionics Division; Navigation Instrumentation and Display Branch (NAVAIR 5337)
- Crew Systems Division; Cockpit/Cabin Requirements and Standards Branch (NAVAIR 5313)

U. S. Army, Army Electronics Command
Avionics Laboratory, Fort Monmouth, New Jersey
- Instrumentation Technical Area (AMSEL-VL-I)

The Joint Army Navy Aircraft Instrumentation Research Program objective is: To conduct applied research using analytical and experimental investigations for identifying, defining and validating advanced concepts which may be applied to future, improved Naval and Army aircraft instrumentation systems. This includes sensing elements, data processors, displays, controls and man/machine interfaces for fixed and rotary wing aircraft for all flight regimes.

NOTICE

Change of Address

Organizations receiving JANAIR Reports on the initial distribution list should confirm correct address. This list is located at the end of the report just prior to the DDC Form 1473. Any change in address or distribution list should be conveyed to the Office of Naval Research, Code 461, Washington, D. C. 20360, Attn: JANAIR Chairman.

Disposition

When this report is no longer needed, it may be transmitted to other organizations. Do not return it to the originator or the monitoring office.

Disclaimer

The findings in this report are not to be construed as an official Department of Defense or Military Department position unless so designated by other official documents.

ABSTRACT

A mathematical model that positions and moves a variable sized 23 pin joint articulated stick-man in a crewstation environment is presented. The model simulates the motion of pilots in a given cockpit configuration after testing the gross reach capability required by a task. It utilizes a non-linear optimization technique to position and orient the joints, analyzes the viewing capability after the operation and detects body intersections with the seatback during the task.

KEYWORD LIST

Cockpit

Design

Geometry

Human

Man-Model

Minimization

Non-Linear

Optimization

Performance

Simulation

TABLE OF CONTENTS

LIST OF ILLUSTRATIONS

1.0 INTRODUCTION

The Cockpit Geometry Evaluation project has as its goal the development of a digital computer program which would evaluate the geometry of proposed crewstation designs. The man-model will be used to evaluate the geometric configuration of the crewstation in terms of the crew's physical characteristics and capabilities.

PHASE REQUIREMENTS

There will be six phases to the development. Each, of one year's duration, will result in a successively greater detailed description of anthropometric characteristics and capabilities of the pilot (Figure 1).

In Phase I, a "baseline" man-model will be developed, using a skeletal frame consisting of stick or line links intersecting at "pin"-joints with specified kinds of link movement originating from the joints.

To simplify the problem for Phase I, attention is restricted to an aircraft pilot's station. For the present development, the copilot will be immobile and of fixed dimension. Furthermore, both pilot and copilot will be operating from a seated position.

In Phase II, skin volumes of rectilinear or circular section will be added to the above "pin-joint stick-man."

Phase III will provide some force and control grasping capability to the "pilot" and incorporate the "preferred" positions for control grasping and force application.

Phase IV will allow for finger dexterity and excursion capability to specified joints of the pilot.

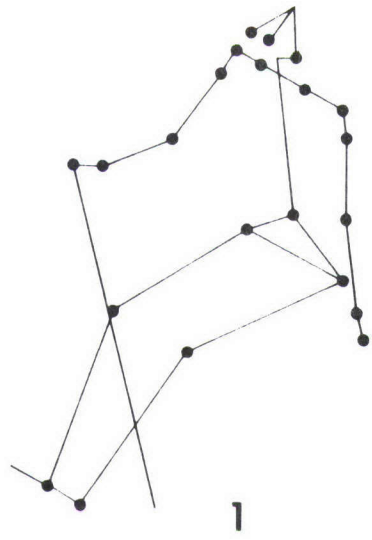

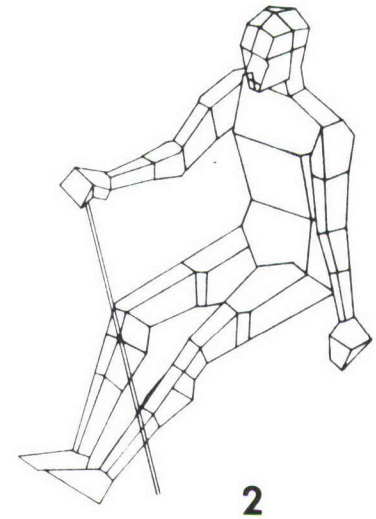

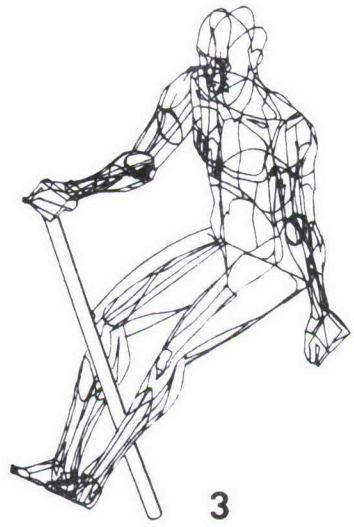

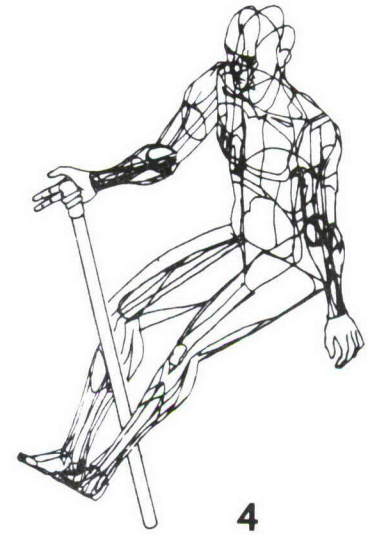

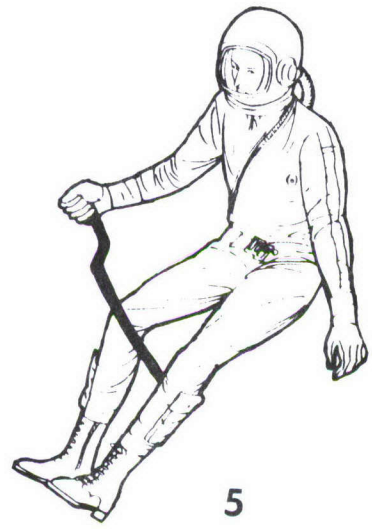

Figure 1. 6-Year Plan

In Phase V, additional force vector variables and initial energy expenditure variables will be incorporated into the "pilot's" range of capability.

Finally, Phase VI will provide a "skin" deformation capability and the final energy expenditure variables will be added to the model.

During each of the Phases, refinements in definitions of cockpit dimensions, display-control locations and control shapes will be made. In addition, validations will be performed to test the hypothesis that the pilot model's positions and movements do not depart "significantly" from those of human pilots.

EVALUATION DESCRIPTION

In order to make the evaluation more meaningful, the computerized man-model (when all project phases are complete) should be able to evaluate a cockpit design in terms of:

(1) Any human anthropometric combination of link sizes between the first and ninety-ninth percentile

(2) Any set of pilot task sequences

The computerized man-model will accommodate any set of cockpit dimensions and control shapes as well as any set of cockpit-induced new movement restrictions due to seats, harnesses, panels and clothing.

In addition, the computerized man-model will supply constructive, consistent, and reproducible predictions concerning:

(1) Display and Control Accessibility - Is it possible for the "pilot" to view a cockpit display (such as an altimeter on the control panel or a specific area in the windscreen) and can he also "see" what he is doing while reaching for a control?

(2) Control Actuation - Is it possible for the "pilot" to operate or can his appendages be placed in the proper orientation for "handling" the control, given the accessibility of the control?

(3) Pilot Workload - Over any given set of tasks, how much "energy" is expended by the pilot; how much "work" is done by the pilot in terms of the body mass displacements and distances traveled by each link; and what is the amount of visual "activity" as measured by head and eye deflections?

(4) Interference - Is there physical or visual interference occurring between the pilot and the cockpit structure or equipment during a task to be performed? The pilot's body and personal equipment will also be considered as possible obstructions.

(5) Suggested Areas for Design Change - In order to make the cockpit physically compatible with pilot capabilities, the computerized man-model will specify why a task is infeasible. This will suggest that a change be made in the cockpit design or procedures.

2.0 SUMMARY

2.1 PROJECT DESCRIPTION

The problem is to develop, over a period of six years, a computerized man-model as a means of evaluating competing designs of aircraft crewstations. Specifically, this is to be accomplished by determining the ability of any size of crewman to reach or view the controls and displays of his crewstation. Interference with projecting parts of the cockpit during the motion is also to be determined. These determinations are to be made by simulating the movements of a human pilot during the execution of various tasks in the crewstation environment by means of a mathematical model programmed for the computer. When given the trajectories and/or orientations of the pilot's extremities (e.g., the hands), this model is to predict the trajectories and orientations of the remaining body segments.

The project objectives for Phase I, therefore, are the following:

a) Develop a math-model and an associated computer program to position and move a 23-pin-joint stick-man in three dimensions.

b) Develop validation procedures and criteria to assess the "reality" of model positions and movements compared to actual pilot movements.

c) Satisfy the requirements of Phase I of the project by supplying useful predictions concerning:

- Display-control accessibility
- Control actuation
- Workload in terms of energy expended, body mass displacements, and distances traveled by the flight crew's eyes and each flight crew appendage
- Visual interferences between the flight crew and the cockpit structure/equipment and physical interferences between flight crew appendages and the seatback.

- Design changes required to make the cockpit subsystem compatible with flight-crew physical capabilities.

2.2 RESULTS

The present model relies on optimization theory to find the body segment trajectories and orientations by minimizing a cost (objective) function. This cost function is assumed to express the amount of effort required by the crew-man to achieve a given body configuration. Total mass displacement and visual interference that occur during the task motion are analyzed after the simulation of a task.

A version of the man motion-model that simulates a human torso and right arm system has been completed. An experimental motion model for the upper body (torso, arms, and head) has also been developed. The current upper body model provides for all body structural constraints except the joint angular limits.

2.3 CONCLUSIONS

The end result of the Phase I Cockpit Geometry effort is a working experimental model of human motion. It appears suitable for use as a comparative tool in limited cockpit geometry evaluation studies. It also appears suitable as a baseline for further research and development aimed at obtaining the fully applicable man-model desired.

2.4 RECOMMENDATIONS

(1) The design of the present model reflects what may be a highly simplified view of the way human pilots move during execution of a task. Therefore additional data on human motion should be gathered to aid in the formulation of better mathematical and physical hypotheses concerning human motion.

(2) More research on the modeling problem is needed to insure accuracy and stability in the model. The baseline man-model is flexible enough to incorporate changes in mathematical or physical hypotheses that might result from this research. Full advantage of this flexibility should be taken by devoting much of the Phase II effort toward major improvements in motion-model formulation.

3.0 DISCUSSION

3.1 ASSUMPTIONS AND NOTATION

The labelling of points on the stick-man is presented in Figure 2 for the purposes of this document.

Task motions are performed in an incremental fashion, a task being defined by moving terminal body segments (e.g., the hands) a step at a time toward the control points for these segments. Solutions are obtained for the Euler angles that define the stick-man's configuration at each step by using optimization with non-linear constraints. Trajectories for the intermediate body segments at each step are calculated from the Euler angles. Here, an underlying assumption is that human motion can be simulated by obtaining solutions in a step-wise manner and using interpolation to obtain body configurations intermediate to the calculated ones. Also, since time is not actually a parameter in the present model, it is assumed that the motion is performed with constant velocity so that discrete time values may be assigned to positions along the motion trajectory of the body.

The main assumptions of the overall model and the notation that applies to Figure 2 are as follows:

ASSUMPTIONS

(1) The stick-man (Figure 2) is initially placed in the cockpit so that the eye reference point coincides with location P_7. Since initial link lengths and orientations are given (with respect to the preceding joint or point), the other P_j are calculable with respect to P_7.

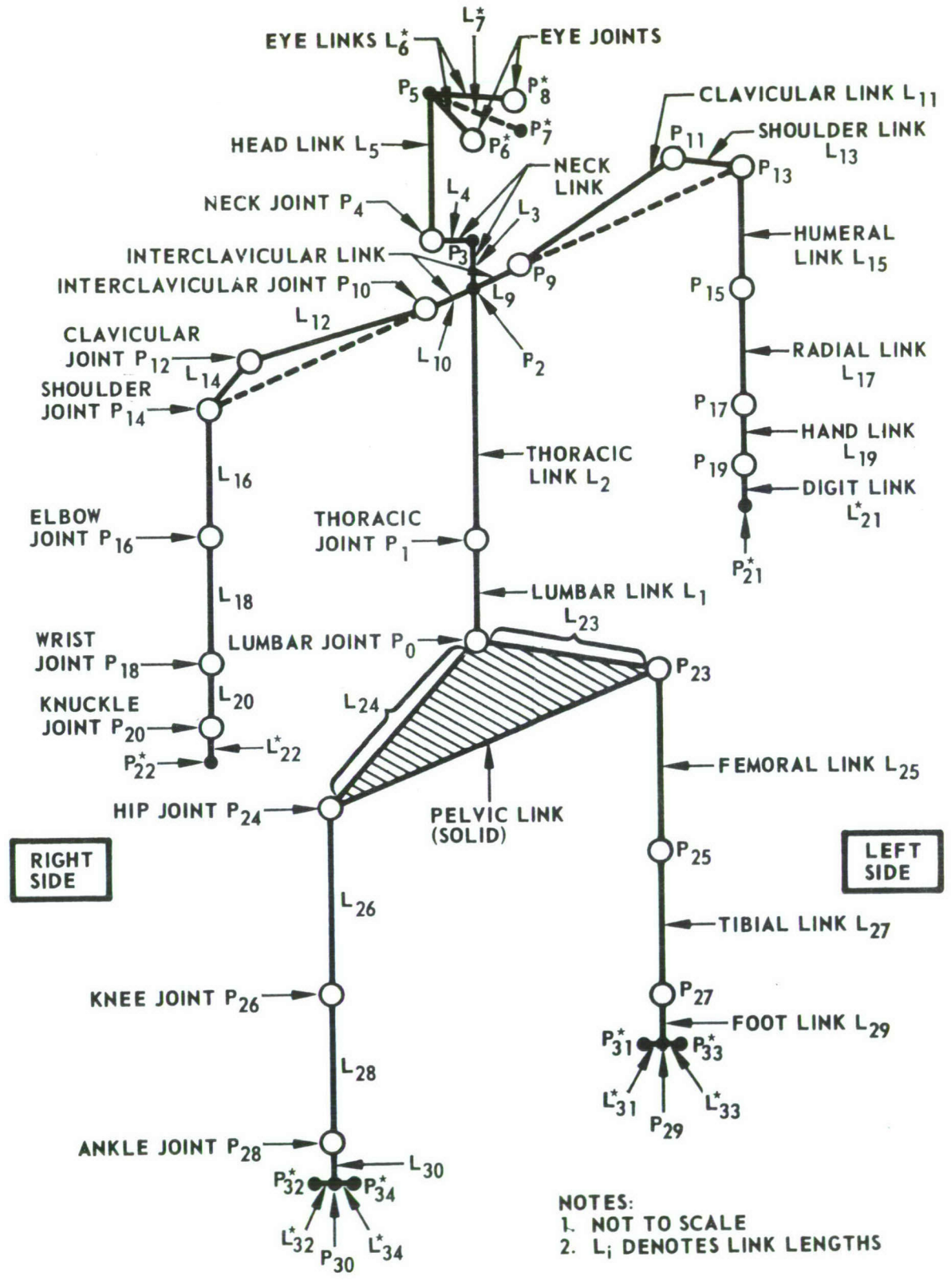

Figure 2. 23 Joint Man-Model Link Nomenclature

(2) In particular, the location P_o is found and P_o becomes the fixed origin for all movements of the stick-man thereafter. (Thus the locations P_j are again determined with respect to the new origin. All cockpit locations are calculated with respect to P_o.)

(3) A task is given (i.e., a specific total body movement from an initial terminal joint position to a final terminal joint position) specifying:

a) Final terminal joint locations (each P_j*).
b) New orientations for each terminal link of length L_i*.
c) A time value to achieve the final position.
d) A time value to remain in the final position.
e) A cockpit location or plane area at which the eyes are to focus.

(4) The legs can be ignored for the Phase I model, leaving only the upper torso, head, and arms to consider.

NOTATION

(1) Let P_j denote the location relative to P_o of point j, where j ranges from j = 0 to j = 34 (e.g., P_o = (0,0,0)).
(2) Let L_i denote the length of Link i. Link i is the line or polygonal line connector between two adjacent junctions (points and/or joints).
(3) For terminal points, j is restricted to the values j = 6, 7, 8, 21, 22, 31, 33, 32, 34 only (for j = 6, 7, 8, 21, 31, 33, 32, 34, j is an interior point).
(4) Let P_2 denote the location relative to P_o at the top of spine point defined as the midpoint of the line (P_9,P_{10}) intersecting the polygonal line (P_1,P_3).
(5) Let P_3 denote the location of the junction occurring between joints P_2 and P_4.

(6) Let P_5 denote the location of the junction occurring at the intersection of the polygonal lines (P_4,P_6) and (P_4,P_8).

(7) Let P_7 denote the midpoint of the line (P_6,P_8) between the eye joints.

(8) Let (P_{32},P_{34}) be the line with length $L_{32} + L_{34}$ and endpoints P_{34} (toe), P_{32} (heel), and with midpoint P_{30} (right foot);
Let (P_{31},P_{33}) be the line with length $L_{31} + L_{33}$ and endpoints P_{33} (toe), P_{31} (heel), and with midpoint P_{29} (left foot).

3.2 REACH ANALYSIS

The Reach Analysis is concerned with determining, in a gross manner, if a prescribed task is with BOEMAN-I's (Figure 3) reach. That is, are BOEMAN-I's link dimensions and joint angular limits such that he can simultaneously position the palm joints of each hand at the task prescribed locations without rising from the seated position. (It is assumed that the lumbar joint (J_o) is fixed and immobile.)

To this end, two problems are formulated:

(a) Is the task feasible?

(b) If not, redefine the task control locations for the hands to insure task feasibility.

The solution to the latter problem allows the motion model to proceed and identify any additional difficulties that could occur such as in body orientation or viewing ability.

NOTATION

A = length of lumbar link (ℓ_1)

B = length of thoracic link (ℓ_2)

C_1 = boundary surface: range of J_o, ($J_1 = 0$)

C_2 = boundary surface: range of J_o, ($J_1 = \pm \beta$)

C_3 = boundary surface: range of J_1, ($J_o = \pm \alpha$)

h = $r \sin\delta$

$P1$, $P2$ = two mutually exclusive portions of R3

r = inner radius of spine region

R = outer radius of spine region = sum of ℓ_1 and ℓ_2

r_i = radius of inner concentric sphere of hand regions

$$r_i = \frac{\ell_{10,}}{2} \quad i = \begin{cases} 1 \text{ left hand} \\ 2 \text{ right hand} \end{cases}$$

R_i = radius of outer concentric sphere of hand regions

$$i = \begin{cases} 1 \text{ left hand} \\ 2 \text{ right hand} \end{cases}$$

$R1$ = right hand region

$R2$ = left hand region

$R3$ = spine region

(x,y,z) = top of spine point

(x_o,y_o,z_o) = initial top of spine point

(x_1,y_1,z_1) = left palm control point

(x_2,y_2,z_2) = right palm control point

(x_3,y_3,z_3) = J_1 at extreme left side

(x_4,y_4,z_4) = J_1 at extreme right side

(x_5,y_5,z_5) = point in $R1 \cap R2$

(x_6,y_6,z_6) = $\begin{Bmatrix} A \sin\alpha \cos\gamma \\ A \sin\alpha \sin\gamma \\ A \cos\alpha \end{Bmatrix}^T$ $0 \leq \alpha < \pi/2$, $0 \leq \gamma \leq \pi$

(x_m, y_m, z_m) = midpoint of (x_1, y_1, z_1) + (x_2, y_2, z_2)

α = J_o angle limit

β = J_1 angle limit

γ = $\cos^{-1}\left(\frac{A + B\cos\beta}{\gamma}\right)$

δ = $90 - \alpha - \gamma$

ϵ = angle of spine in x-y plane

$\emptyset$ = empty set

$\cap$ = intersection symbol

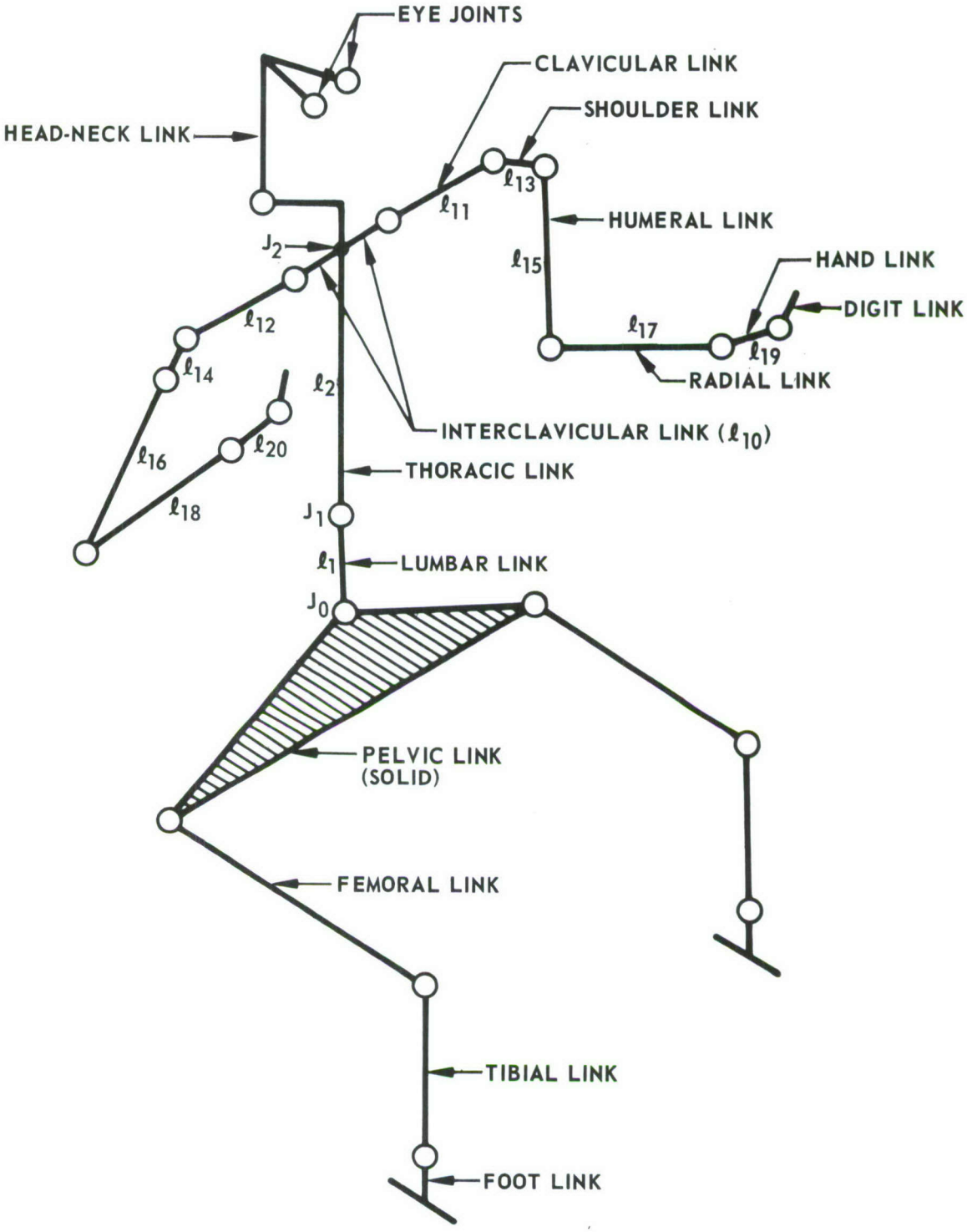

Figure 3. 23-Joint Man-Model Link Nomenclature

3.2.1 Task Feasibility

It is natural to consider the top of the spine (J_2) as the key to task feasibility, for it is a juncture of three body systems: the spine, the right arm, and the left arm. By fixing the palm joints at the task locations, with the lumbar joint already fixed relative to the seat reference point, the task is deemed feasible if these body systems yield at least one common top of spine location.

Consequently, three regions will be defined with respect to the fixed points of each body system, each describing the locus of points that the top of the spine can assume. Then task infeasibility will be assumed if it is not possible to exhibit a point in the mutual intersection of the three regions.

HAND REGIONS

The Right Hand Region, denoted R1, is defined as the set of all points that the top of the spine can assume, given that the right palm joint is at the corresponding task control point. It is defined by the two extreme arm positions, encompasses virtually all possible arm positions (see Figure 5). The left hand region, denoted R2, is defined in a similar manner (see Figure 6).

For BOEMAN-I, given a fixed palm location, the effective distance between the palm and any top of spine location ranges from zero to the sum of the link lengths for the corresponding arm system (including the shoulder). It is necessary to determine bounds on this distance that closely approximate those encountered by human beings.

For a lower bound, it is assumed that some positive radius, r_i, equal to one half the length of the interclavicular link (about an inch) be used, where i = 1, 2 denote the left and right arm system, respectively.

(1) $$r_i = \frac{\ell_{10}}{2}, \quad i = 1,2$$

A small positive distance is assumed because it is not possible to touch the top of the spine with either palm due to the intervening flesh.

For an upper bound, it is necessary to choose a radius that represents a compromise between forward arm reach and lateral arm reach. In the former, the links between the top of the spine and the shoulder do not contribute to the maximum forward reach; however, they contribute fully in the latter. This holds of course, when one neglects the rotational capability of the spine. However, a twisting spine (torso) tends to give added reach to only one arm system and compensates by decreasing the reach of the other arm system. Thus to approximate maximum reach of human beings, and effect a "balanced" reach capability, it is assumed that the maximum distance is given by radius R_i,

$$R_1 = +\left(\left(\frac{\ell_{10}}{4}\right)^2 + \left(\ell_{11} + \ell_{13} + \ell_{15} + \ell_{17} + \ell_{19}\right)^2\right)^{\frac{1}{2}}$$

(2)
$$R_2 = +\left(\left(\frac{\ell_{10}}{4}\right)^2 + \left(\ell_{12} + \ell_{14} + \ell_{16} + \ell_{18} + \ell_{20}\right)^2\right)^{\frac{1}{2}}$$

(See Figure 4).

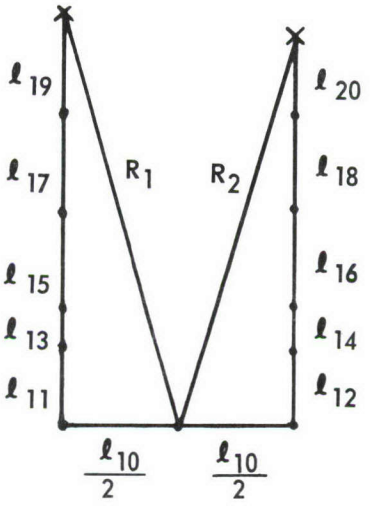

Figure 4. Maximum Reach for Each Arm System (Top View)

Thus, R_i corresponds to an extended arm position and r_i corresponds to a contracted arm position. This will include virtually all other arm positions since they must have a reach distance (from the palm to the top of the spine) between R_i and r_i.

The right hand region (Figure 5) then, can be described as the volume between the two concentric spheres, both centered at the right palm control point, (x_2,y_2,z_2) and with radii r_2,R_2. Then

$$(3)\quad R1 = \{(x,y,z) \mid r_2^2 \leq (x-x_2)^2 + (y-y_2)^2 + (z-z_2)^2 \leq R_2^2\}$$

Similarly, the left hand region (Figure 6) can be described as the volume between the two concentric spheres, both centered at the left palm control point (x_1,y_1,z_1) and with radii r_1,R_1. Then

$$(4)\quad R2 = \{(x,y,z) \mid r_1^2 \leq (x-x_1)^2 + (y-y_1)^2 + (z-z_1)^2 \leq R_1^2\}$$

SPINE REGION

The spine region, denoted R3, is defined as the set of all points that the top of the spine can assume given that the lumbar joint (J_o) is fixed and that the links in the spine system may not violate any joint angular limits.

R3 differs from R1 and R2 in that it is a more accurate (and more complex) region. This is because it is necessary for this region to contain no points that cannot be attained by appropriate rotation angle values on the spine joints, with specified link lengths. It is generated in terms of distinct bounding surfaces C_1,C_2,C_3.

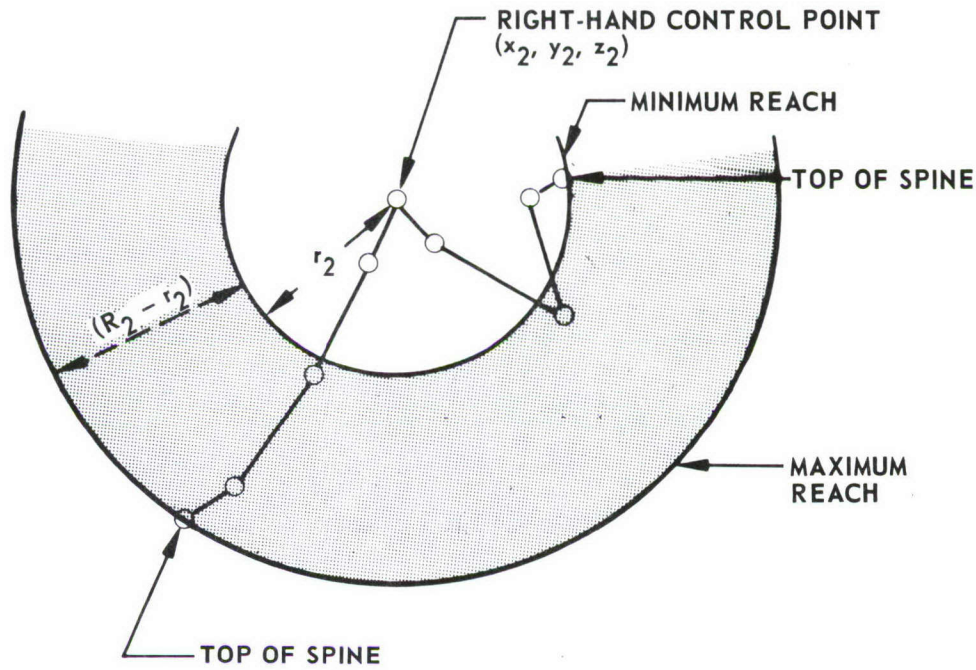

Figure 5. Right-Hand Region, R1—Cross Section of a Portion of Two Concentric Spheres

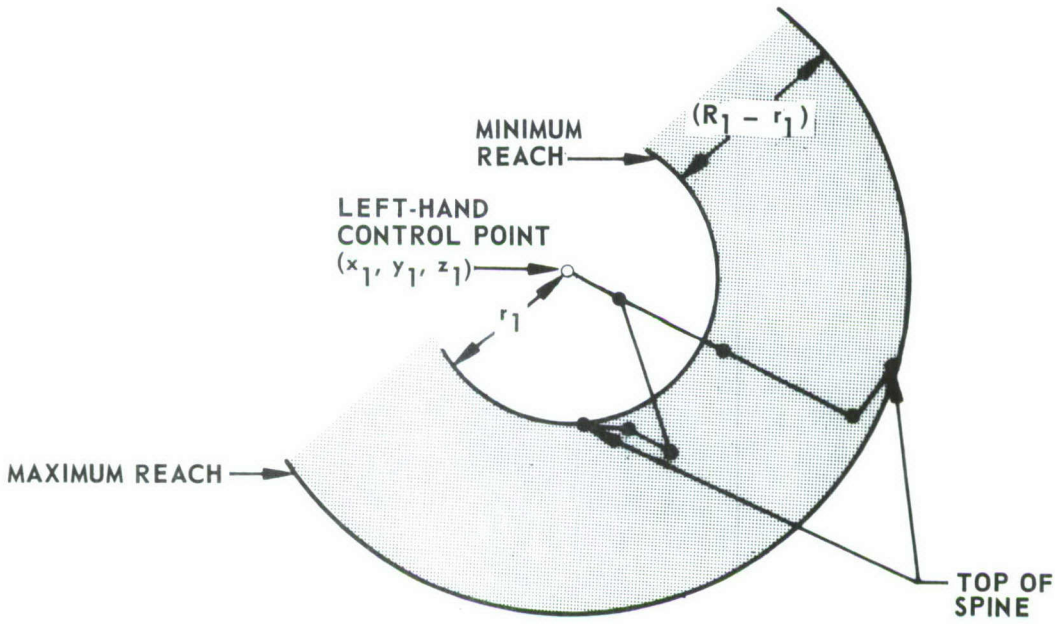

Figure 6. Left-Hand Region, R2 – Cross Section of a Portion of Two Concentric Spheres

The first bounding surface (C_1) is developed by considering the effect of angular deviation in the lumber joint J_o (Figure 7) with zero deviation in the thoracic joint (J_1)

Let R = A+B, the sum of link lengths in the spine

α = maximum angular deviation from the standard (upright) position (left and right)

J_2= (x, y, z)

J_o= (0, 0,0)

Then the top of the spine point is on the surface C_1 if and only if

$$(5)\ x^2 + y^2 + z^2 = R^2$$

Subject to:

$$-R \sin\alpha \leq x \leq R \sin\alpha$$

$$0 \leq y \leq R \sin\alpha$$

$$R \cos\alpha \leq z \leq R$$

Next, consider the fixed extreme limits that the middle joint (J_1) can deviate and the angular deviation of the bottom joint (J_o). The result is the bounding surface C_2

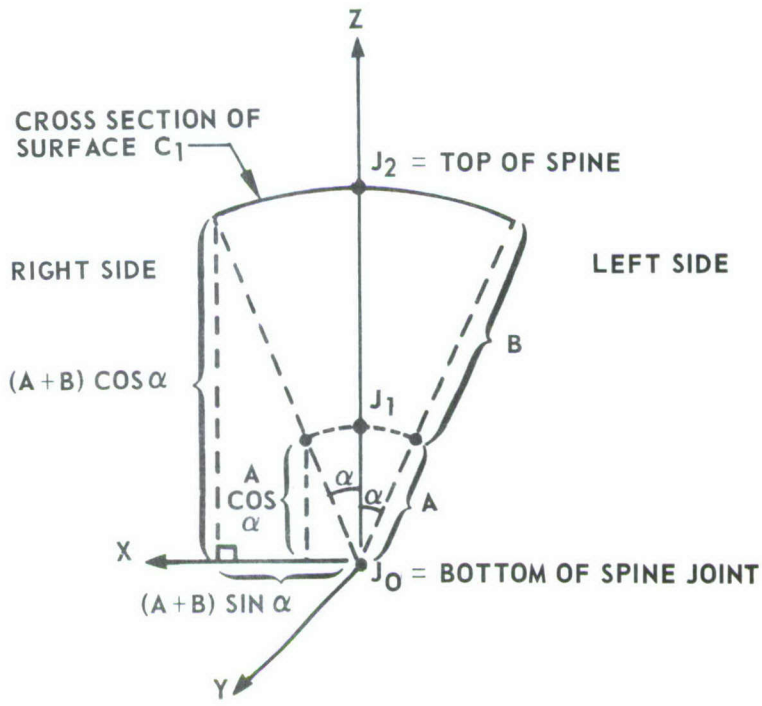

Figure 7 Joint Angular Motion at Bottom Joint–Upper Link at Zero Deviation

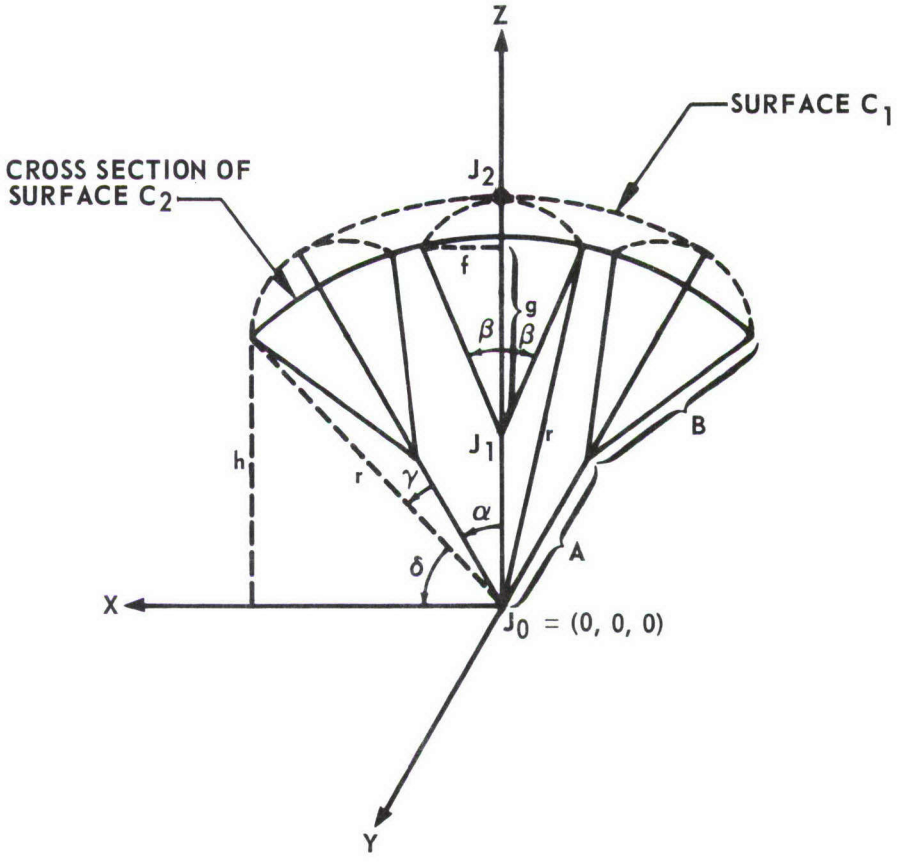

Figure 8. Joint Angular Motion at Bottom Joint – Upper Link in Extreme Deviation

Let β = maximum angular deviation from the standard (upright) position towards x-axis

$f = B \sin\beta$

$g = B \cos\beta$

r = radius of inner curve C_2 and

$$r^2 = f^2 + (g+A)^2$$

$$= B^2 \sin^2\beta + (A + B\cos\beta)^2$$

$$= B^2 \sin^2\beta + A^2 + 2AB\cos\beta + B^2\cos^2\beta$$

$$r^2 = A^2 + B^2 + 2AB\cos\beta$$

Then the top of the spine is on surface C_2 if and only if

$$x^2 + y^2 + z^2 = r^2 \tag{6}$$

subject to

$$-r\cos\delta \leq x \leq r\cos\delta$$

$$0 \leq y \leq r\cos\delta$$

$$h \leq z \leq r$$

where $h = r\sin\delta$, $\delta = 90 - \alpha - \gamma$,

$$\gamma = \cos^{-1}\left(\frac{A + B\cos\beta}{r}\right)$$

(using the law of cosines, $B^2 = A^2 + r^2 - 2Ar\cos\gamma$

$$= A^2 + (A^2 + 2AB\cos\beta + B^2) - 2Ar\cos\gamma$$

$$\therefore r\cos\gamma = A + B\cos\beta)$$

Finally, consider the extreme limits that the bottom joint (J_o) can deviate and the angular deviation of the middle joint (J_1). The result is boundary surface C_3.

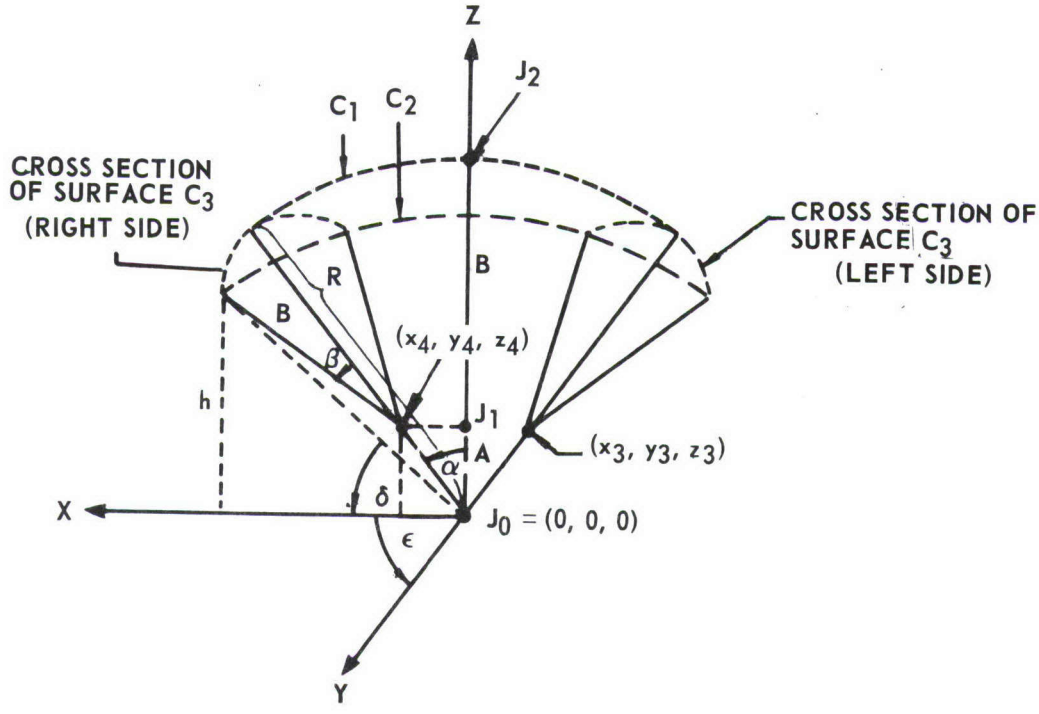

Figure 9. Joint Angular Motion at Middle Joint–Lower Link in Extreme Deviation

On the positive x-axis, the top of the spine point is on surface C_2 if

$$(7) \quad (x-x_4)^2 + (y-y_4)^2 + (z-z_4)^2 = B^2$$

where

$$\left.\begin{aligned} x_4 &= A \sin\alpha \cos\epsilon \\ y_4 &= A \sin\alpha \sin\epsilon \\ z_4 &= A \cos\alpha \end{aligned}\right\} \quad \begin{aligned} 0 \leq \epsilon \leq \pi \\ 0 \leq \alpha \leq \pi/2 \end{aligned}$$

and subject to:

$$R \sin\alpha \leq x \leq \cos\delta$$

$$R \sin\alpha \leq y \leq \cos\delta$$

$$h \leq z \leq R \cos\alpha$$

On the negative x-axis, the top of the spine point is on surface C_3 if

$$(8) \quad (x-x_3)^2 + (y-y_3)^2 + (z-z_3)^2 = B^2$$

where

$$\left.\begin{aligned} x_3 &= -A \sin\alpha \cos\epsilon \\ y_3 &= +A \sin\alpha \sin\epsilon \\ z_3 &= A \cos\alpha \end{aligned}\right\} \quad \begin{aligned} 0 \leq \epsilon \leq \pi \\ 0 \leq \alpha \leq \pi/2 \end{aligned}$$

and subject to:

$$-r \cos\delta \leq x \leq -R \sin\alpha$$

$$R \sin\alpha \leq y \leq r \cos\delta$$

$$h \leq z \leq R \cos\alpha$$

where $h = r \sin\delta$ (see (6))

Then C_1, C_2 and C_3 together, describe the spine region. It has been assumed that the seated pilot is constrained by a seat back. Thus C_1 are defined for $y \geq 0$ only. Region R_3 is depicted in Figure 10.

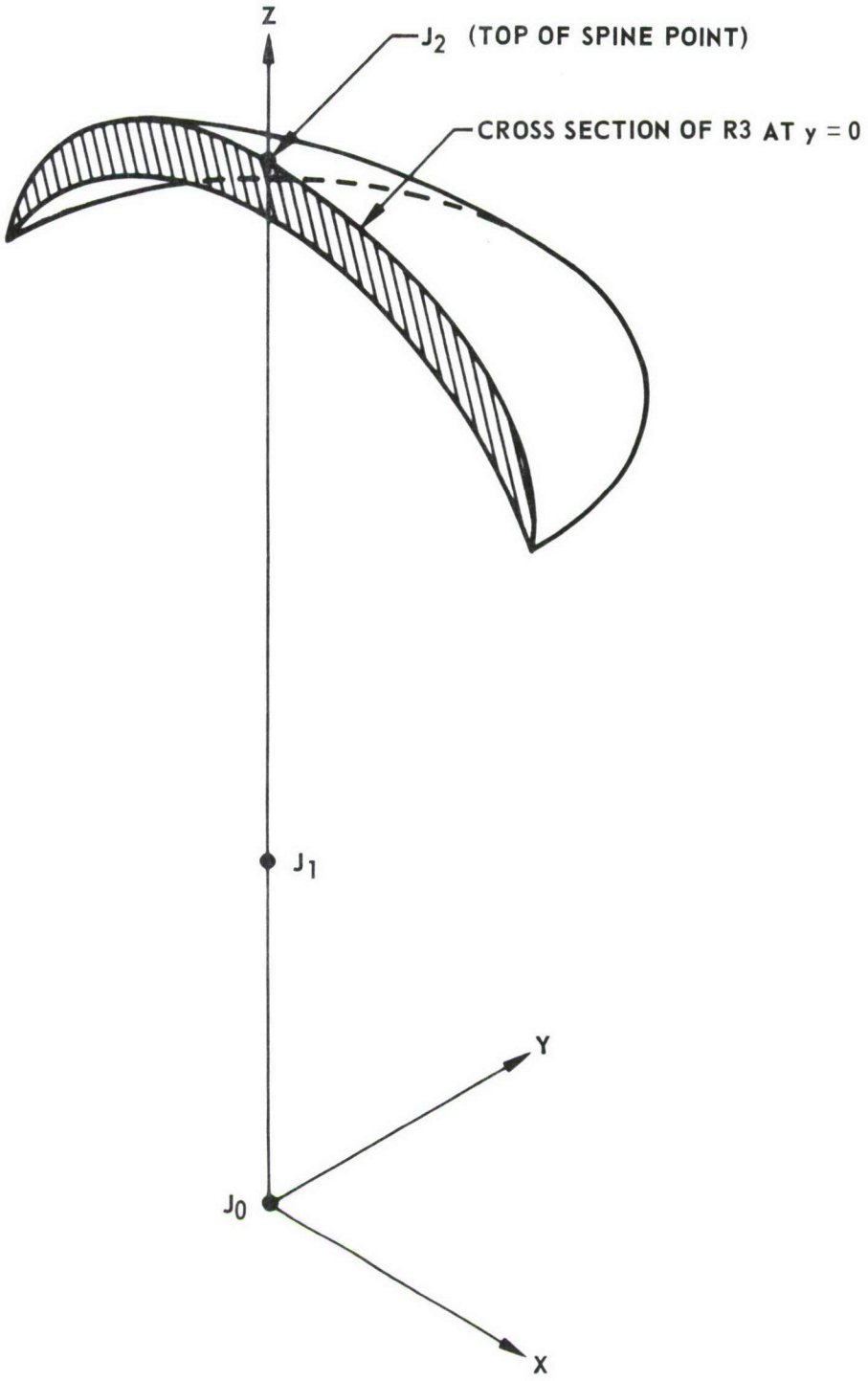

Figure 10. Region 3–Feasible Region for Top-of-Spine Locations

SPINE REGION PARTITION

In order to exhibit a point in the mutual intersection, it is convenient to partition R3 as in Figure 11 , into two mutually exclusive portions P1,P2 such that:

Portion P1 is constrained by

$$P1 = \left\{ (x,y,z) \;\middle|\; \begin{array}{l} r^2 \le x^2+y^2+z^2 \le R^2 \\ -R \sin\alpha \le x \le R \sin\alpha \\ 0 \le y \le R \sin\alpha \\ R\cos\alpha \le z \le R \end{array} \right\} = \left\{ (x,y,z) \;\middle|\; \begin{array}{l} r^2 \le x^2+y^2+z^2 \le R^2 \\ \\ 0 \le y \\ R\cos\alpha \le z \end{array} \right\}$$

Portion P2 is constrained by

$$P2 = \left\{ (x,y,z) \;\middle|\; \begin{array}{ll} r^2 \le x^2+y^2+z^2 & (x_6 = A \sin\alpha \cos\gamma \\ (x-x_6)^2 + (y-y_6)^2 + (z-z_6)^2 \le B^2; & y_6 = A \sin\alpha \sin\gamma \\ -R\cos\delta \le x \le R\cos\delta & z_6 = A\cos\alpha \\ 0 \le y \le R\cos\delta & 0 \le \alpha < \pi/2 \\ r\sin\delta \le z \le R\cos\alpha & 0 \le \gamma \le \pi \;) \end{array} \right\}$$

These portions allow for a method of solution using an optimization technique (MINUM) for which it is necessary that upper and lower bounds be available for each of the unknown quantities (x,y,z). Hence, the overdetermined constraint set is used for P1.

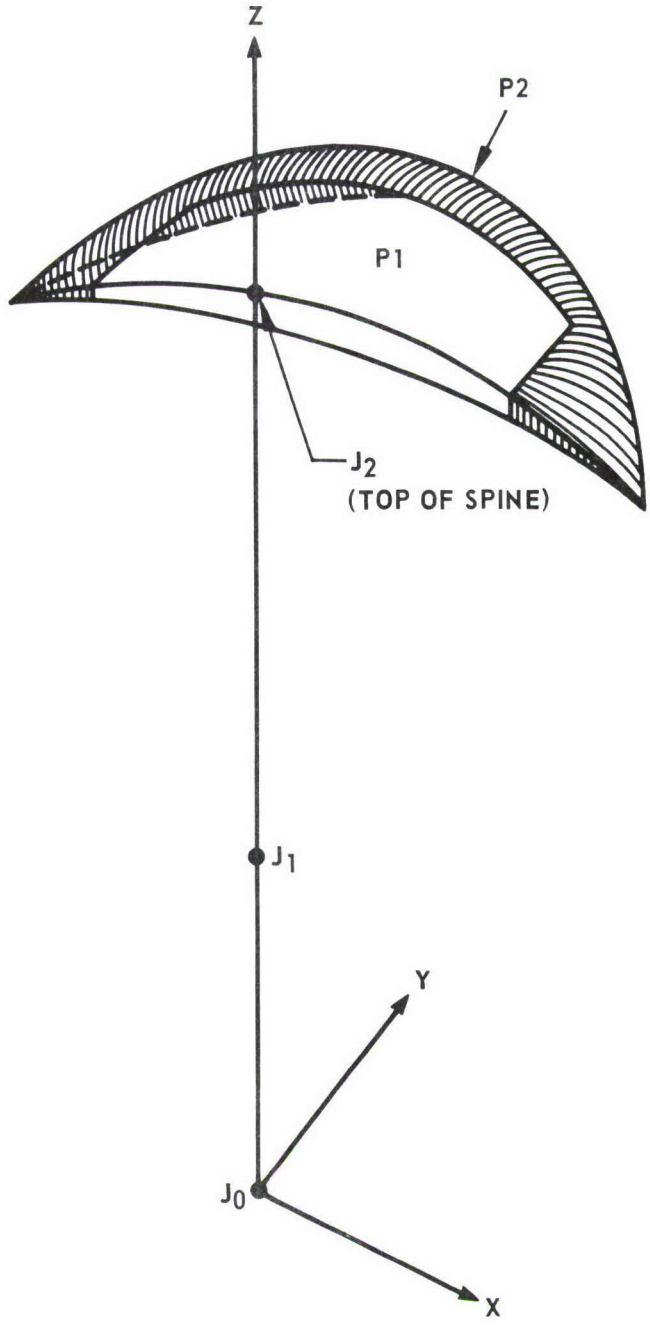

Figure 11. Region 3 Partition

METHOD OF SOLUTION

The regions, R1, R2, R3, are tested for a mutual intersection under the assumption that if such an intersection exists a feasible top of spine location is calculable, and thus the task is feasible.

It is sufficient to show that the mutual intersection region exists by calculating a point belonging to all three regions simultaneously.

Finding a feasible top of spine location requires that there exists a point (x,y,z) in Regions 1 and 2 and in at least one of the portions P1, P2 of Region 3. If the mutually intersecting regions have a finite volume, there are an infinite number of feasible candidates. Thus, it is necessary to select one point from the infinite set. To do this, a nonlinear objective function is set up which acts as a rating system among the feasible candidates and selects by some criteria a "best" one. The criteria will be to find a top of spine location as close as possible to the top of spine position at the beginning of the task (denoted as (x_o,y_o,z_o)).

(11) Objective Function 1: $(x - y_o)^2 + (y - y_o)^2 + (z - z_o)^2$

This method has the advantages of ease in formulation, and computational rapidity using a computer.

In general, two problems are solved, each corresponding to a protion of R3. They are:

(12) Problem 1: Minimize (objective function 1)
subject to R1, R2, and Pi, i = 1,2

This results in at most two (true) minimum values for objective

function 1, with the top of the spine located in at most two of the portions. For definiteness, a top of spine location (x,y,z) is chosen such that if k_1, k_2 are the minima for problems 1 and 2, let $k = \text{MIN}(k_1,k_2)$. It follows that (x,y,z), corresponding to this minimum, is a feasible top of spine point.

Corresponding to (12)

(12a) Minimize

$$(x - x_o)^2 + (y - y_o)^2 + (z - z_o)^2$$

subject to

$$(1a)\quad r_1^2 \le (x-x_1)^2 + (y-y_1)^2 + (z-z_1)^2 \le R_1^2 \quad (R2)$$

$$(2a)\quad r_2^2 \le (x-x_2)^2 + (y-y_2)^2 + (z-z_2)^2 \le R_2^2 \quad (R1)$$

$$(3a)\quad r^2 \le x^2 + y^2 + z^2 \le R^2$$

$$(4a)\quad -R\sin\alpha \le x \le R\sin\alpha \qquad (P1)$$

$$(5a)\quad 0 \le y \le R\sin\alpha$$

$$(6a)\quad R\cos\alpha \le z \le R$$

(12b) Minimize

$$(x - x_o)^2 + (y - y_o)^2 + (z - z_o)^2$$

subject to

$$(1b)\quad r_1^2 \le (x-x_1)^2 + (y-y_1)^2 + (z-z_1)^2 \le R_1^2 \quad (R2)$$

$$(2b)\quad r_2^2 \le (x-x_2)^2 + (y-y_2)^2 + (z-z_2)^2 \le R_2^2 \quad (R1)$$

$$(3b)\quad r^2 \le x^2 + y^2 + z^2$$

$$(4b)\quad (x-x_6)^2 + (y-y_6)^2 + (z-z_6)^2 \le B^2$$

$$(5b)\quad -r\cos\delta \le x \le r\cos\delta \qquad (P3)$$

$$(6b)\quad 0 \le y \le r\cos\delta$$

$$(7b)\quad r\sin\delta \le z \le R\cos\alpha$$

where $(x_6,y_6,z_6) = (A\sin\alpha\cos\gamma\ ,\ A\sin\alpha\sin\gamma\ ,\ A\cos\alpha)$,

$0 \le \gamma \le \Pi$
$0 \le \alpha < \Pi/2$

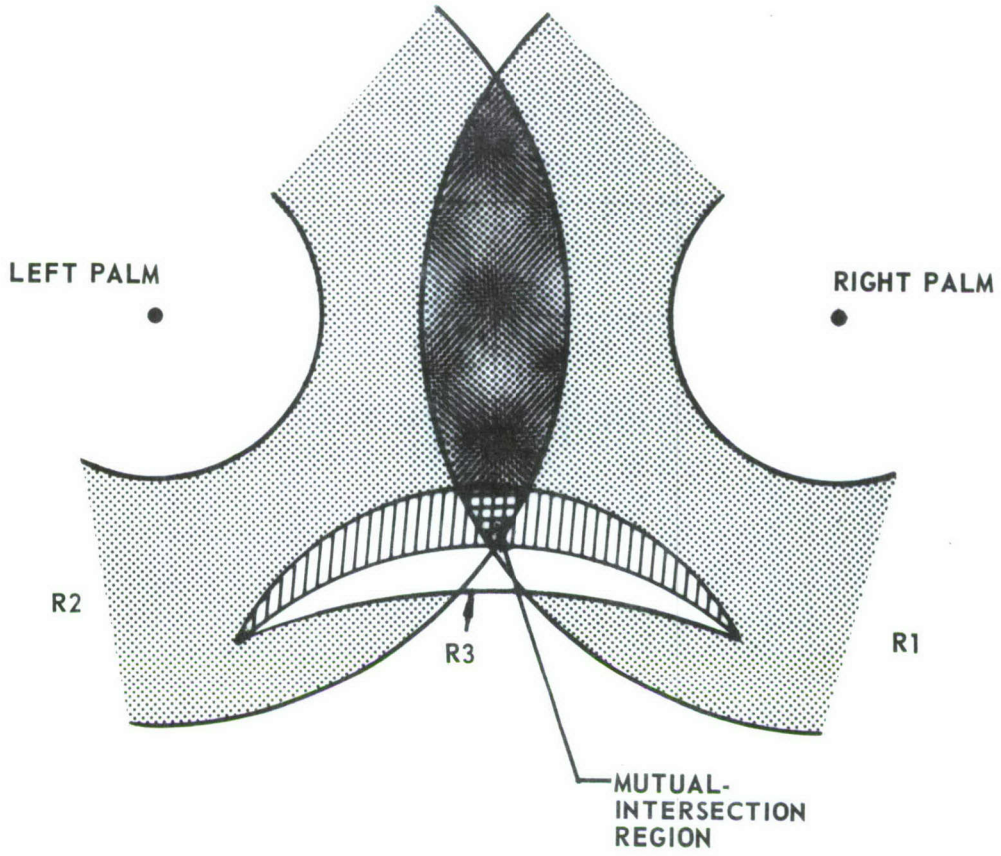

Figure 12. Region of Mutual Intersection

3.2.2 Task Modification

If a task is infeasible then there is no mutually intersecting region for the top of the spine. The task is then modified by redefining a new pair of palm locations which can be reached with the link configuration under consideration. This allows for subsequent evaluation of the modified task which "closely" resembles the original one. Ideally, a task should be modified so that each change of palm position could be an indicator of required control change. This would provide a useful design tool. However, relocation of a control must be considered in relation to all other controls which may be operated simultaneously with it. Thus, it is beyond the scope of this analysis to provide a true indicator of design changes on the basis of a given task.

The modification of the task provides that a top of spine location be calculated so that the resulting body position is as "close" as possible to the original task defined control locations. With some alterations, the method used in determining task feasibility can be used here, provided that the left and right palm locations are redefined appropriately so that a non-empty mutual intersection region exists. It is important to emphasize that the two palm control locations of a task have equal importance and one must have both palms positioned as specified in order to consider a task accomplished.

The cases where a mutual intersection region does not exist are of two types: (a) R1 and R2 have a mutual intersection; (b) R1 and R2 are disjoint.

Case I: INTERSECTION OF HAND REGIONS

This case allows for

$$R1 \cap R2 \cap R3 = \phi$$
$$R1 \cap R2 \neq \phi$$

It is necessary to find the top of spine location within R3 closest to the intersection of R1 and R2 and once chosen, designate new palm locations in the direction of the original ones and at a distance R_i from the top of spine location. This will allow BOEMAN-I to perform the task in the same manner as any original task.

Suppose (x_5, y_5, z_5) represents any point in the mutual intersection of Regions 1 and 2. Let a spherical surface of radius r be coincident with the under-surface of Region 3 (see Figure 13). There exists some (x_5, y_5, z_5) whose distance to the sphere of radius r is a minimum. This shortest distance is embodied in the normal from this point to the sphere at $(\hat{x}, \hat{y}, \hat{z})$. It is determined if $(\hat{x}, \hat{y}, \hat{z})$ is on Region 3 or below it. If $(\hat{x}, \hat{y}, \hat{z})$ is on Region 3, then let $(x, y, z) = (\hat{x}, \hat{y}, \hat{z})$. If $(\hat{x}, \hat{y}, \hat{z})$ is below Region 3, let $(x, y, z) = (r \cos\delta \cos\eta, r \cos\delta \sin\eta, r \sin\delta)$ using the rim portion of Region 3 as the circle of closest location to (x_5, y_5, z_5) where $\delta = \tan^{-1} \frac{y}{x}$ and is the angle formed by (x, y, z), $(0,0,0)$ and $(\hat{x}, \hat{y}, \hat{z})$.

Thus, mathematically, let

$$(13) \quad (x_5 t_1)^2 + (y_5 t_1)^2 + (z_5 t_1)^2 = r^2$$
$$(x_5 t_2)^2 + (y_5 t_2)^2 + (z_5 t_2)^2 = r^2$$

where

$$t_1 = + \sqrt{\frac{r^2}{x_5^2 + y_5^2 + z_5^2}}, \quad t_2 = -t_1$$

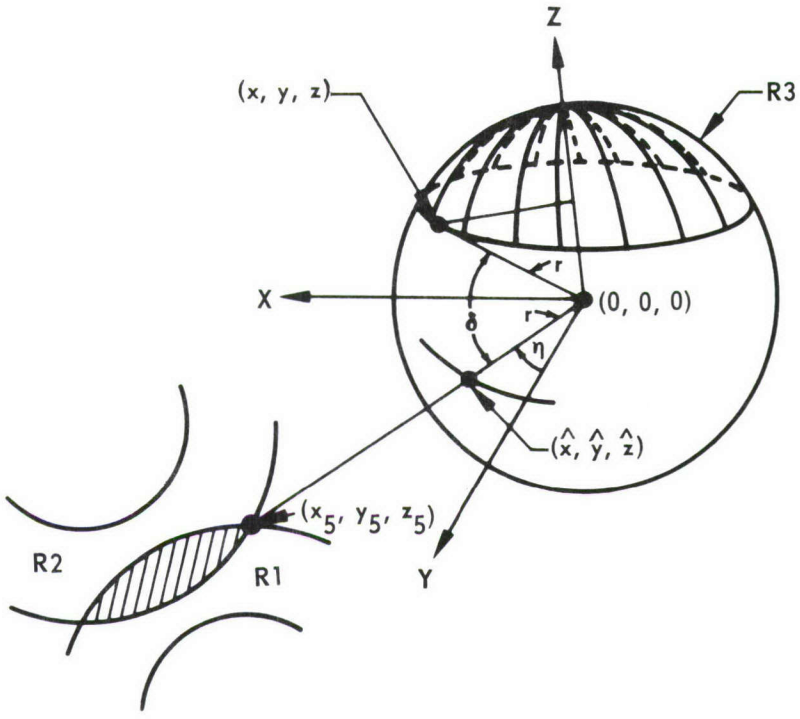

Figure 13. Case I: $R1 \cap R2 \neq \phi$

t_1 and t_2 represent factors, both between ± 1, which determine two points on the sphere forming a line that extends to meet (x_5,y_5,z_5) and is normal to the sphere.

Choosing the t_j for which

$$\text{Min}\left[\sqrt{(x_5-x_5t_1)^2 + (y_5-y_5t_1)^2 + (z_5-z_5t_1)^2}\ ,\ \sqrt{(x_5-x_5t_2)^2 + (y_5-y_5t_2)^2+(z_5-z_5t_2)^2}\right]$$

holds, let

$$(\hat{x},\ \hat{y},\ \hat{z}) = \text{Min}\ (x_5t_i,\ y_5t_i,\ z_5t_i).$$

If $(\hat{x},\ \hat{y},\ \hat{z}\ )$ satisfies the constraints

$$-r\cos\delta \le \hat{x} \le r\cos\delta$$

$$0 \le \hat{y} \le r\cos\delta$$

$$r\sin\delta \le \hat{z} \le r$$

then $(x,y,z) = (\hat{x},\hat{y},\hat{z})$ is the chosen top of spine location,

otherwise,

(14) let $(x,y,z) = (r\cos\delta\cos\eta\ ,\ r\cos\delta\sin\eta\ ,\ r\sin\delta)$,

$$\eta = \tan^{-1}\left(\frac{\hat{y}}{\hat{x}}\right)$$

Thus the problem is to find an (x_5,y_5,z_5) for which

(15) $(x_5-x)^2 + (y_5-y)^2 + (z_5-z)^2$ is minimized

subject to

$$r_2^2 \le (x_5-x_2)^2 + (y_5-y_2)^2 + (z_5-z_2)^2 \le R_2^2 \qquad \text{(Region 1)}$$

$$r_1^2 \le (x_5-x_1)^2 + (y_5-y_1)^2 + (z_5-z_1)^2 \le R_1^2 \qquad \text{(Region 2)}$$

$$\text{MIN}\left[(x_2-R_2),(x_1-R_1)\right] < x_5 \leq \text{MAX}\left[(x_2+R_2),(x_1+R_1)\right]$$

$$\text{MIN}\left[(y_2-R_2),(y_1-R_1)\right] < y_5 \leq \text{MAX}\left[(y_2+R_2),(y_1+R_1)\right]$$

$$\text{MIN}\left[(z_2-R_2),(z_1-R_1)\right] < z_5 \leq \text{MAX}\left[(z_2+R_2),(z_1+R_1)\right]$$

Using (14), one generates a feasible top of spine location and redefines (x_1,y_1,z_1), (x_2,y_2,z_2), (palm control positions) to be

$$(16)\begin{cases}\hat{x}_i = x + (x_i-x)\cdot S_i \\ \hat{y}_i = y + (y_i-y)\cdot S_i \\ \hat{z}_i = z + (z_1-z)\cdot S_i\end{cases} \qquad S_i = \frac{R_i}{((x_i-x)^2+(y_i-y)^2+(z_i-z_2)^2)^{1/2}}$$

CASE II: DISJOINT HAND REGIONS

Case II assumes:

$$R1 \cap R2 = \emptyset$$

It is necessary to find a top of spine location closest to each of the original palm locations and redefine the palms as in Case I.

Because both of the locations have equal weight, the midpoint between them is chosen and the top of spine is to be positioned within region R3 and closest to this mid-point (See Figure 13).

If

$$(17)\quad (x_m, y_m, z_m) = \left[\left(x_2 + \frac{x_1-x_2}{2}\right), \left(y_2 + \frac{y_1-y_2}{2}\right), \left(z_2 + \frac{z_1-z_2}{2}\right)\right]$$

then for Regions 1, 2 and portion P1 or P2 of Region 3,

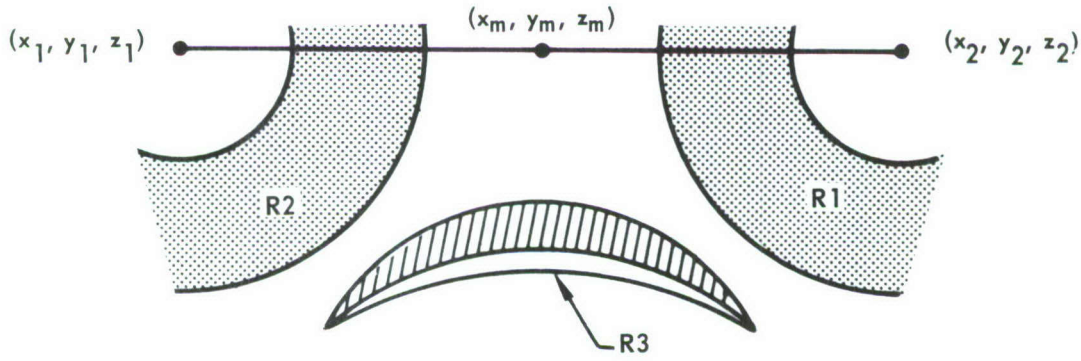

Figure 14. Case II: R1 ∩ R2 = ∅

using the method of 3.2.1,

(18) Objective Function 2: $(x-x_m)^2 + (y-y_m)^2 + (z-z_m)^2$

and

(19) Problem i': Minimize (Objective Function 2)

subject to

$$Pi',i' = 1,2$$

Choosing the smallest of the two resulting minima, the top of spine location with respect to (x_m,y_m,z_m) is found and Pi' are as defined in (9), (10).

The task is redefined, using the top of spine location (x,y,z) found as in (16).

3.3 THE MOTION MODEL

This section mathematically describes the model for the simulation of human motion by a geometric stick-figure. This method generalizes easily to handle rigid skin volumes. The problem is formulated in a general way in the Section 3.3.1 where vector functions and differentiation formulas relevant to the model are presented. In Sections 3.3.2, and 3.3.3, the mathematical formulation of the model is more specific. The human motion problem is presented as an optimization problem with non-linear constraints.

NOTATION

B = a vector function on the vector z of variable Euler angles, defining a stick-man body configuration in the vector x, of position coordinates of link-connecting points on the stick-man, $x = B(z)$.

C_{I_i} = a Euclidean coordinate system whose center is at P_{I_i}; if $I_i \neq 0$, the z-axis of this system has the direction of $P_{I_i} - P_{I_{i-1}}$, and if $I_i = 0$, the axes of C_{I_i} define the cockpit reference axes.

F = an objective function for optimization. $F(z) = \hat{f}(z) + h(z)$ where $\hat{f}$ and h are defined below.

$\hat{F}$ = the composition of F with a vector function G, which is defined below, to get an objective function in terms of a vector y, $\hat{F}(y) = F(G(y))$.

f = an objective function for optimization defined directly in terms of the stick-man body configuration position vector $x = B(z)$.

$\hat{f}$ = the composition of f with B to get a function directly in terms of Euler angles, $\hat{f}(z) = F(B(z))$.

G = the vector function that removes angular constraints from the stick-man problem by expressing z as a function of an unconstrained vector y, $z = G(y)$.

h = an objective function for optimization defined directly in terms of the Euler angle vector z.

$\left\{ I_i \right\}_{i=1}^{m}$ = a monotone increasing sequence of non-negative integers defining a sequential array of link-connecting points on the stick-man (e.g., the joint locations from the bottom of the spine to the top of the spine, then on out to the tip of the right arm).

L_{I_i} = the distance of $|P_{I_i} - P_{I_{i-1}}|$, i.e. the length of link I_i

M_j^i = $\prod_{K=j}^{i} T_{I_K}$

P_{I_i} = a 3 dimensional vector giving the coordinates of position vector I_i on the stick-man ($1 \leq i \leq m$).

P_{I_i,I_j} = a column vector representing the point P_{I_i} in the C_{I_j} - system.

$q(K)$ = a non-negative integer such that z_K is an angle for rotation $T_{I_{q(K)}}$

S = an arbitrary point in the cockpit.

S_{I_i} = a column vector representing S in the C_{I_i} system.

T_{I_i} = a 3-space rotation matrix giving the orientation of system C_{I_i} relative to $C_{I_{i-1}}$.

t_{I_i} = the translation vector $\begin{bmatrix} 0 \\ 0 \\ L_{I_i} \end{bmatrix}$, expressed in system C_{I_i}, used to translate between $C_{I_{i-1}}$ and C_{I_i}.

$\mathbf{x}$	=	$B(z)$
y	=	a vector such that $z = G(y)$.
z	=	a vector composed of all the variable Euler angles in the stickman, arranged in some order.
z_K	=	a component of z.
$\theta_{I_i}, \phi_{I_i}, \psi_{I_i}$	=	the Euler angles used to calculate T_{I_i}.

3.3.1 Coordinate Systems

Until now it has been convenient to refer to the locations $P_i (i = 1,\ldots, 34)$ of the link - connectors on the stick-man as Euclidean vectors in a coordinate system based at P_o; however, a means of expressing the orientation of each body segment (e.g., forearm, hand, etc.) is needed. For example, the right shoulder (joint 14) not only has location P_{14}, but also an orientation that expresses the amount by which the humeral link - Link 16 - is oriented in space relative to the right clavicular link - Link 14.

To express the orientations of joints and, in fact, all link - connecting points, local coordinates are used for the points P_i on the stick-man. Orientations then become 3-space rotations, which are used in affine transformations to change the system relative to which any point in the cockpit is expressed as a Euclidean vector.

For exactness, let $\{I_i\}_{i=1}^{m}$ be a sequence of non-negative integers defined as the indices of the points P_{I_i} in a sequentially ordered subsystem of the stick-man, e.g., the sequence 0,1,2,10,12,14,16,18,20,22 (where m = 10) corresponds to the thorax-right arm system (Figure 2). Since the cockpit reference system is based at P_o, always choose $I_1 = 0$. Define coordinate systems C_{I_i} $(i = 1,\ldots, m)$ centered at P_{I_i}, each with z-coordinates (z) - axis parallel to link I_i. Then for two adjacent points I_{i-1} and I_i, systems $C_{I_{i-1}}$ and C_{I_i} are centered at a distance L_{I_i} apart, with the orientation of C_{I_i} relative to $C_{I_{i-1}}$ expressed by the matrix:

$$T_{I_i} = T(\theta_{I_i}, \varphi_{I_i}, \psi_{I_i}) = (T_{jk}(\theta_{I_i}, \varphi_{I_i}, \psi_{I_i})).$$

θ_{I_i}, ϕ_{I_i}, and ψ_{I_i} are "quasi-Euler" angles, to be interpreted as indicated in Figure 15. The entries for the matrix $T(\theta,\phi,\psi) = (T_{JK}(\theta, \phi, \psi))$ are

$$
\begin{aligned}
T_{11} &= \cos\theta \cos\phi \cos\gamma + \sin\phi \sin\gamma \\
T_{21} &= \cos\theta \sin\phi \cos\gamma - \cos\phi \sin\gamma \\
T_{31} &= -\sin\theta \cos\gamma \\
T_{12} &= \cos\theta \cos\phi \sin\gamma - \sin\phi \cos\gamma \\
T_{22} &= \cos\theta \sin\phi \sin\gamma + \cos\phi \cos\gamma \\
T_{32} &= -\sin\theta \sin\gamma \\
T_{13} &= \sin\theta \cos\phi \\
T_{23} &= \sin\theta \sin\phi \\
T_{33} &= \cos\theta \quad ,
\end{aligned}
$$

where $\gamma = \phi - \psi$.

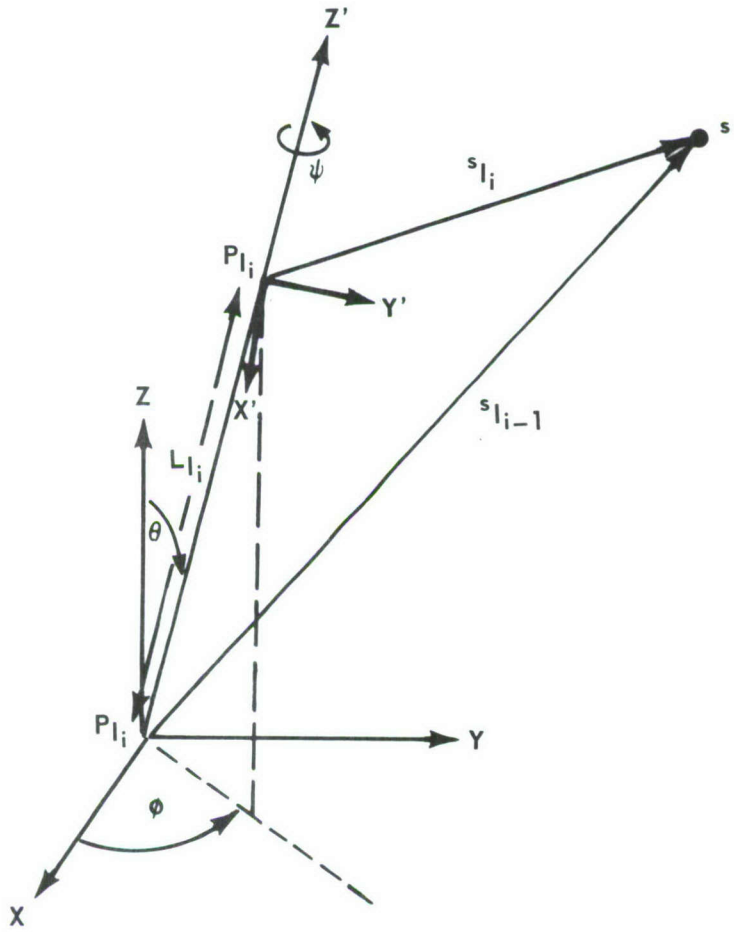

Figure 15. Coordinate System Transformation

Thus if S is a point in the cockpit expressed in system C_{I_i} as a column-vector S_{I_i}, $S_{I_{i-1}}$ is found by means of the affine transformation A_{I_i} given by

$$S_{I_{i-1}} = A_{I_i} S_{I_i} = T_{I_i} (S_{I_i} + t_{I_i}) \text{ where}$$

$$t_{I_i} = \begin{bmatrix} 0 \\ 0 \\ L_{I_i} \end{bmatrix}$$

To form $S_{I_{i-2}}$, two affine transformations are applied in succession to get

$$S_{I_{i-2}} = A_{I_{i-1}} A_{I_i} S_{I_i}$$

$$= T_{I_{i-1}} (T_{I_i} (S_{I_i} + t_{I_i}) + t_{I_{i-1}})$$

$$= T_{I_{i-1}} T_{I_i} S_{I_i} + T_{I_{i-1}} T_{I_i} t_{I_i} + T_{I_{i-1}} t_{I_{i-1}} .$$

Proceeding in this way, when $j < i$, then

$$S_{I_j} = \prod_{K=j+1}^{i} A_{I_K} S_{I_i}$$

$$= \prod_{K=j+1}^{i} T_{I_K} S_{I_i} + \sum_{q=0}^{i-(j+1)} \prod_{K=j+1}^{i-q} T_{I_K} t_{I_{i-q}}$$

Note that if S_{I_J} is P_{I_i, I_j}, (the coordinate center of C_{I_i} in C_{I_j} - coordinates), then

$$P_{I_i,I_j} = \prod_{K=j+1}^{i} T_{I_K} \begin{bmatrix} 0 \\ 0 \\ 0 \end{bmatrix} + \sum_{q=0}^{i-(j+1)} \prod_{K=j+1}^{i-q} T_{I_K} t_{I_{i-q}} .$$

Letting $M_i^j = \prod_{K=i}^{j} T_{I_K}$, P_{I_i}, I_i may be expressed

(2) $$P_{I_i}, I_j = \sum_{q=0}^{i-(j+1)} M_{j+1}^{i-q} \; t_{I_{i-q}}$$, and in particular

(3) $$P_{I_i} = P_{I_i,0} = \sum_{q=0}^{i-2} M_2^{i-q} \; t_{I_{i-q}}$$

The expression for S_{I_j} in terms of S_{I_i} now becomes

(4) $S_{I_j} = M_{j+1}^i \; S_{I_i} + P_{I_i,I_j}$; and for $j = 1$, (i.e., $I_j = 0$)

(5) $S_o = M_2^i \; S_{I_i} + P_{I_i}$, an expression giving S in C_o - coordinates.

In particular,

(6) $P_{I_i} = M_2^i \; t_{I_i} + P_{I_{i-1}}$

It will be seen in later sections that expressions for finding gradients of vector functions of the rotation angles θ_{I_i}, ϕ_{I_i}, and ψ_{I_i}, discussed before, are desired for the present stick-man model. In setting forth these expressions, only the orientation angles that may vary during a movement of the stick-man are treated as variables; some of the points I_i have 0 degrees of freedom of orientation (e.g., for $I_i = 3$ or 5 (Figure 2); these are link-connectors but not joints), others 2 or 3 degrees of freedom. In some joints, such as 18 (see Figure 2), the angle ψ will remain constant. For this reason, a parameter vector z is defined whose components are the orientation angles in the stick-man that may vary during a given motion or task. If only the right arm subsystem is to move during a task, the components of z are chosen as the

variable angles in the right-arm joints; here the defining sequence is $I_1 = 0$, $I_2 = 1$, $I_3 = 2$, $I_4 = 10$, $I_5 = 12$, $I_6 = 14$, $I_7 = 16$, $I_8 = 18$, $I_9 = 20$, and $I_{10} = 22$.

System C_o is the cockpit reference system and stays fixed by definition. Referring to Figure 2, fixed orientations are defined for systems C_1, C_2, and C_{10} (centered at P_1, P_2, and P_{10}, respectively), and for C_{14} (P_{12} is treated as a link-connector but not a joint for the present). For the body segments centered at links 12, 16, 18, 20 and 22 respectively, 2, 3, 2, 2, and 1 degrees of freedom of orientation are allowed. With one exception, whenever 2 degrees of freedom are allowed, orientation angles θ and ϕ are used. (The z-axis of system C_{I_i} is rotated counter-clockwise an angle θ_{I_i} degrees in a plane ϕ_{I_i} degrees (counter-clockwise) from the x-axis of system $C_{I_{i-1}}$.) The exception is joint 16, where θ_{18} and ψ_{18} are used (i.e., the C_{18} z-axis is rotated θ_{18} degrees from the C_{16} z-axis, always in a fixed plane in C_{16}, and resulting xy-system is twisted counter-clockwise by an angle ψ_{18}). Thus the parameter vector for this example is

$$z = (\theta_{12}, \phi_{12}, \theta_{16}, \phi_{16}, \psi_{16}, \theta_{18}, \psi_{18}, \theta_{20}, \phi_{20}, \theta_{22}).$$

Given a component variable z_K of z, q(k) is selected from the domain of the sequence $\{I_i\}_{i=1}^{m}$ such that z_K is a variable in transformation $T_{I_{q(K)}}$ (i.e., z_K represents one of the degrees of freedom for link $I_{q(K)}$). z_K apperas as a variable only in $T_{I_{q(K)}}$, thus for any matrix product

M_i^j, the partial derivative with respect to z_K is

$$(7)\qquad \frac{\partial M_i^j}{\partial z_K} = \begin{cases} M_i^{q(K)-1} \dfrac{\partial T_{I_{q(K)}}}{\partial z_K} M_{q(K)+1}^j & \text{if } i \le q(K) \le j \\ 0 \quad \text{matrix} & \text{otherwise,} \end{cases}$$

where differentiation is done componentwise on the matrix $T_{I_{q(K)}}$ and any product of the form M_i^{i-1} is interpreted as the multiplicative identity matrix.

It is convenient to reformulate (7) for recursive differentiation of M_2^i $(i = 2,\ldots,m)$ as

$$(8)\qquad \frac{\partial M_2^i}{\partial z_K} = \begin{cases} \dfrac{\partial M_2^{i-1}}{\partial z_K} T_{I_i} & \text{if } q(K) < i \\ M_2^{i-1} \dfrac{\partial T_{I_i}}{\partial z_K} & \text{if } q(K) = i \\ 0 \quad \text{matrix} & \text{if } q(K) > i\ . \end{cases}$$

Using (8), the partial derivatives of the point locations P_{I_i} as functions of the parameters z_K can now be expressed according to the recursive formula

$$(9)\qquad \frac{\partial P_{I_i}}{\partial z_K} = \frac{\partial M_2^i}{\partial z_K} t_{I_i} + \frac{\partial P_{I_{i-1}}}{\partial z_K} \quad \text{as i goes from 2}$$

to m. Use has been made of the fact that t_{I_i} is a constant vector and

$$\frac{\partial P_o}{\partial z_K} = 0 \quad \text{for all K.}$$

Gradient formulas for vector functions of the parameter vector z, e.g. the gradient of the point-vector P_{12} on the stick-man, will now be exhibited.

Suppose that z has n component variables z_K (K = 1,...,n). For each point P_{I_i} in a system defined by a sequence $\{I_i\}_{i=1}^{m}$, formula (3) (or (6)) defines a mapping (vector function) from z to P_{I_i}. This mapping is differentiable, with partial derivatives given by (9). By constructing the vector $x = \begin{bmatrix} \cdot \\ \cdot \\ \cdot \\ (P_{I_i})_j \\ \cdot \\ \cdot \\ \cdot \end{bmatrix}$, where $(P_{I_i})_j$ is the j-th component of of P_{I_i} (j = 1,2,3; i = 2,...,m), it is possible to define a differentiable mapping $B : z \longrightarrow x = B(z)$. In this instance x is written as

$$x = \begin{bmatrix} x_1 \\ \cdot \\ \cdot \\ \cdot \\ x_i \\ \cdot \\ \cdot \\ \cdot \\ x_p \end{bmatrix} = \begin{bmatrix} B_1(z) \\ \cdot \\ \cdot \\ \cdot \\ B_i(z) \\ \cdot \\ \cdot \\ \cdot \\ B_p(z) \end{bmatrix}, \text{ where}$$

p = 3 x (number of movable points in the system), e.g. in the example of the movable right-arm system, the vectors P_o, P_1, P_2, and P_{10} would not be used in constructing x.

Corresponding to the mapping B, for each value $\bar{z}$ for which $\bar{x} = B(\bar{z})$ is defined, an nxp (gradient) matrix $B_z(\bar{z})$ is obtained according to

(10) $B_z(\bar{z}) = (\bar{B}_{ij}) = \left(\left(\frac{\partial B_j}{\partial z_i} \right)_{z=\bar{z}} \right)$. Each entry $\left(\frac{\partial B_r}{\partial z_K} \right)_{z=\bar{z}}$ has the form $\frac{\partial (P_{I_i})_j}{\partial z_K}$ (the derivative of the j-th component (j = 1,2, or 3) of P_{I_i}) for some i and j corresponding to r, hence may be found using (9).

The preceding analysis will be used in section 3.3.3, where a gradient-projection optimization model for the stick-man is given, in the following way: If $f: x \longrightarrow f(x)$ is a differentiable function on the x-space defined above (e.g. an objective function), then for each $\bar{x} = B(\bar{z})$ a function $\hat{f}$ is defined on z-space by $\hat{f}(\bar{z}) = f(B(\bar{z}))$; if the gradient of f is f_x, the gradient $\hat{f}_z$ of $\hat{f}$ at $z = \bar{z}$ is given by

(11) $\hat{f}_z(\bar{z}) = B_z(\bar{z})\, f_x(\bar{x}) = B_z(\bar{z})\, f_x(B(\bar{z}))$;

here $\hat{f}_z$ and f_x are, as usual, column vectors.

3.3.2 Constraints

As mentioned before, the problem of simulating human motion is that of finding the trajectories of all body segments when a task is defined by giving the trajectories of the body segments at the extremities. Solutions to the problem are restricted by placing limitations on the stick-man's motion due to human body constraints (angular constraints) and environmental constraints. Thus the constraints on the motion problem are of two kinds: Constraints that serve to define a task, and constraints that result from restriction on the freedom of movement of a human pilot. In terms of the mathematics involved, the task-definition constraints are equality constraints and the limiting constraints are inequalities.

TASK DEFINITION

The present formulation of the task definition constraints includes position, orientation, and directional constraints, all of which have been used in the existing model. Position constraints require that certain terminal points on the body reach specified points in the crewstation environment. This is the most important type of constraint in defining a task, hence it is used in all cases. To define such a constraint explicitly, suppose P_{I_m} is a terminal point on the stickman's body. It is required that P_{I_m} match the point C in the cockpit. (C may be either the control point to be reached by P_{I_m} at the end of the task-motion, or an intermediate point along a specified path from the initial value of P_{I_m} to the control point.) $P_{I_m} = P_{I_m}(z)$ is a function of the vector z of Euler angles describing relative body segment orientations and hence, expression (3) in Section 3.3.1 yields the constraint equation:

(12) $P_{I_m}(z) - C = 0$ in terms of z. The condition (12) is

satisfied if and only if the cockpit reference coordinates of P_{I_m} and C are the same.

The orientation and directional constraints are presently applied only at the end of a task-motion, to more completely define the terminal position of the task.

A more precise definition of terminal position in terms of orientation seems necessary because the pilot's body configuration may depend on not only the location of the controls he is to reach, but also the orientations of his hands when grasping the controls. To formulate this, consider the matrix product

$$M_2^m(z) = \prod_{k=2}^{m} T_{I_k}(z).$$

This is the product of all rotations T_{I_k} needed to find the coordinates of a point on terminal body segment I_m in terms of the cockpit reference system based at P_o for the link-system defined in the sequence $\{I_k\}_{k=1}^{M}$.

$M_2^m(z)$ completely defines the orientation of body segment I_m in system C_o. By specifying Euler angles $\bar{\theta}$, $\bar{\varphi}$, and $\bar{\psi}$ corresponding to the required orientation of segment I_m this orientation can be defined by evaluating the rotation matrix

$$T(\bar{\theta}, \bar{\varphi}, \bar{\psi}) = \bar{T}$$

Hence, it is required that

(13) $M_2^m(z) - \bar{T} = 0.$

In practice, it is helpful to limit the number of entries of $M_2^m(z)$ and T actually considered as constraints (see Section 3.3.3). Presently, only the first column of the

matrix equation (13) is used, giving a 3-space vector equation which expresses the condition that the image of the unit vector $\begin{bmatrix}1\\0\\0\end{bmatrix}$ under the rotation $M_2^m(z)$ matches its image under the rotation $\bar{T}$.

Finally, a directional constraint is applied to the problem at the terminal task-motion position by the requirement that the stick-man be able to look at a specified control point. It is required that the line-of-sight match a vector from the eye midpoint of the stick-man to the vision control point. In the present model, we take point P_6 to be the eye midpoint and consider an "eyeball" located at P_6 as an added link of unit length based at P_6. This link has two degrees of freedom, corresponding to the angle θ and direction ϕ of bending of this link away from the z-axis of system C_6 (aligned with the top of the head). In the present model, the labelling system has been modified somewhat for ease of computing; the line-of-sight vector is $P_7 - P_6$, and it is required that this be aligned with $C-P_6$, where C is the vision control point. One way of expressing this is

$$(14)\qquad (P_7(z) - P_6(z)) - \frac{C - P_6(z)}{|C - P_6(z)|} = 0;\ \text{for}$$

purposes of experimentation with various methods, however, the present model requires the inner product of the two unit vectors in (14) to be unity, i.e.,

$$(15)\qquad (P_7(z) - P_6(z)) \cdot \frac{C - P_6(z)}{|C - P_6(z)|} - 1 = 0.$$

This completes the present list of equality constraints as long as inequality constraints are not removed by redefining them as equivalent equality constraints (see Angular Constraints). For a discussion of the results of this

formulation of task - definition constraints to date, see Section 3.3.3.

ANGULAR CONSTRAINTS

According to available data, the constraints on the variable orientation angles in a given joint i have the following form:

$$\lambda_{\phi_i} \leq \phi_i \leq \mu_{\phi_i}$$

$$\lambda_{\theta_i}(\phi_i) \leq \theta_i \leq \mu_{\theta_i}(\phi_i) \tag{16}$$

$$\lambda_{\psi_i} \leq \psi_i \leq \mu_{\psi_i}$$

That is, the lower bounds λ_{ϕ_i} and λ_{ψ_i} are fixed, but the lower bound on θ_i depends on ϕ_i; the same relationship holds for upper bounds.

In terms of the parameter vector z and corresponding stick-man sub-system described by the sequence $\{I_i\}_{i=1}^{n}$, let $I_{q(K)}$ be the link for which z_K is a parameter, as before. Thus z_K is one of

$$\theta_{I_{q(K)}}, \phi_{I_{q(K)}}, \text{ or } \psi_{I_{q(K)}}; \text{ if } z_K = \theta_{I_{q(K)}}, \text{ and}$$

$\phi_{I_{q(K)}}$ is a variable then $z_{K+1} = \phi_{I_{q(K)}}$, and hence the corresponding inequality from (16) is

$$\lambda_K(z_{K+1}) \leq z_K \leq \mu_K(z_{K+1}). \tag{17}$$

If z_K is either $\phi_{I_{q(K)}}$ or $\psi_{I_{q(K)}}$ or if $\phi_{I_{q(K)}}$ is a constant

the inequality takes the form

$$(18) \quad \lambda_K \leq z_K \leq u_K ,$$

with the upper and lower bounds fixed.

As a means of unconstraining the problem, suppose a differentiable transformation, G, is constructed that takes any vector y with real components y_i (i=1,..,n) to a vector z with components z_i (i = 1, ..., n) in such a way that the z_i are bounded as above. Thus G is a differentiable mapping from real n-space (y-space) into the restricted z-space defined by inequalities of the forms (17) and (18). If it also is required that G is a mapping onto restricted z-space, e.g., if (17) and (18) are taken as strict inequalities, the component mappings G_i of G might have the form

$$(17)' \quad \begin{aligned} z_k &= G_i(y) \\ &= \lambda_{z_i}(G_{i+1}(y)) + \\ &= \left[\mu_{z_i}(G_{i+1}(y)) - \lambda_{z_i}(G_{i+1}(y))\right] \left(\tfrac{1}{2} + (1/\pi)\mathrm{Tan}^{-1} y_i\right) \end{aligned}$$

to remove the constraint of equation (17) and

$$(18)' \quad \begin{aligned} z_i &= G_i(y) \\ &= \lambda_{z_i} + (\mu_{z_i} - \lambda_{z_i}) \left(\tfrac{1}{2} + (1/\pi)\ \mathrm{Arctan}\ y_i\right) \end{aligned}$$

to remove the constraint of equation (18). Equations (17)' and (18)' produce an unconstrained problem in y-parameter space (all of n-space), and the components of the transformation G are G_i(i = 1,..., n).

Now consider the function $\hat{f}$ defined by $\hat{f}(z) = f(B(z))$, as in Section 3.3.1. Defining a function F on y-space by $F(y) = \hat{f}(G(y)) = f(B(G(y)))$ yields the gradient formula

$$F_y(\bar{y}) = G_y(\bar{y})\ \hat{f}_z(\bar{z}); \text{ using } \hat{f}_z(\bar{z}) \text{ as given by (11),}$$

$$(19)\quad F_y(\bar{y}) = G_y(\bar{y})\ B_z(\bar{z})\ f_x(\bar{x})$$

$$= G_y(\bar{y})\ B_z(G(\bar{y}))\ f_x(B(G(\bar{y})))$$

for $\bar{y}$ in y-space, where $G_y(\bar{y})$ is the nxn matrix with elements

$$G_{ij} = \left(\frac{\partial G_j}{\partial y_i}\right)_{y = \bar{y}}.$$

If the mapping G has the form given by (17)' and (18)', $G_y(\bar{y})$ is almost a diagonal matrix.

An alternative means of removing the angular constraints as inequalities is to transform them into equivalent equality constraints. The expression for an overall equality constraint is

$$(20)\quad g(z) = \sum_{i=1}^{r} \left[H(\lambda_i - z_i)\cdot(z_i - \lambda_i)^2 + H(z_i - \mu_i)\cdot(z_i - \mu_i)^2\right] = 0$$

where H is the function given by

$$H(x) = \begin{cases} 0 & \text{if } x \leq 0 \\ 1 & \text{if } x > 0; \end{cases}$$

again, if some of the constraint boundaries vary as in (17), the resulting terms in the summation in (20) have the form

$$(21)\quad H(\lambda_i(z_{i+1}) - z_i)\cdot(z_i - \lambda_i(z_{i+1}))^2 +$$

$$H(z_i - \mu_i(z_{i+1}))\cdot(z_i - \mu_i(z_{i+1}))^2 .$$

So far, both formulations (17)' and (20) have been tried. The added complexity inherent in using (18)' or (21) for variable constraint boundaries has eliminated their use in the Phase I motion-model. Formulation (17)' has been emphasized because it automatically eliminates the constraints from consideration; if formulation (20) must be used, there is one more equality constraint to consider in addition to the task definition constraints.

The type of transformation presented in (17)' has been found to work only in a one-arm synthesis model used for experimental work on the overall motion-model. This transformation did not work on the full upper torso model, a deficiency which is probably a result of using the Arctan transformation. An alternative is to use $\sin^2 y_i$ in (17)' in place of $(\frac{1}{2} + (1/\pi)\ \text{Arctan}\ y_i)$; this has been tried on the one-arm model, with performance considerably improved over that of the Arctan version. Since the formulation in (20) has been tried with no success on the upper torso model, (17)' with the $\sin^2$ transformation will be tried on the full man in Phase II.

ENVIRONMENTAL CONSTRAINTS

The work space of the pilot will generally be described as an enclosed convex region bounded by planes and/or spherical segments with the exclusion of certain protrusions of similar geometric description (e.g., control panels, control stick, copilot, etc.). The environmental constraint implied by such a workspace definition is that no part of the pilot's body may travel outside of the workspace. These constraints are not considered in Phase I. For future project phases, it is

expected that each convex constraint body can be represented by no greater than 10 basic elements (plane and spherical segments), and that there will be no more than 36 constraint bodies.

3.3.3 The Objective Function Approach

This section describes the application of optimization theory to the simulated man-motion modeling problem, and the results obtained so far.

Recall the parameter vector z of variable Euler angles used to orient the body segments of a computer - simulated man. A complete description of the entire body configuration in any given position is obtained once the corresponding value of z is known. In the optimization approach, this is obtained by minimizing F(z) subject to the constraints of section 3.3.2, where F is a real-valued function of z which, when minimized, expresses a set of hypotheses about human motion. (For example, F(z) might be the total energy involved in maintaining the body configuration corresponding to z.) Using the penalty function method (see reference 4) to remove the equality constraints from the problem (after the inequalities have been removed by either of the two methods discussed in section 3.3.2), the objective function F is modified by adding to it a penalty function. The Davidon variable metric method of minimization (see references 1 and 2) has been used with some modifications to solve the stick man modeling problem. The modifications: a Fibonacci search (see reference 3) for recovery from cubic interpolation failure, and a unimodality test to ensure success in one dimensional optimization, are both presented in reference 5.

Suppose the objective function is given as the sum of two terms, one defined directly in terms of position coordinates P_{I_i} of the link-connectors, the totality of which make up the vector x as in section 3.3.1, and the other defined in terms of the vector z of orientation angles for the stick-man sub-systems under consideration. Let the two terms be, respectively, the functions f and h. Using the transformations discussed in section 3.3.1 an expression for x in terms of z, $x = B(z)$

is obtained. B is a differentiable mapping and has a gradient matrix given by

$$B_z(\bar{z}) = (\bar{B}_{ij}) \text{ where}$$

$$\bar{B}_{ij} = \left(\frac{\partial B_j}{\partial z_i} \right)_{z=\bar{z}} = \frac{\partial x_j}{\partial z_i},$$

x_j being a component of one of the point-locations P_{I_K} expressed in C_o - coordinates.

The function $f : x \to f(x)$ together with B defines a function $\hat{f} : z \to f(B(z))$ on z. Then the objective function evaluated at a point $\bar{z}$ in parameter-space has the form $F(\bar{z}) = f(B(\bar{z}))+h(\bar{z})$.

Differentiating as in formula (11), the gradient of F at $\bar{z}$ is given by

$$(22)\quad F_z(\bar{z}) = B_z(\bar{z})\, f_x(B(\bar{z})) + h_z(\bar{z})$$

In the case that inequality constraints are removed by use of the mapping G defined in section 3.3.2, the objective function $\hat{F}$ in y-space (defined by $\hat{F}(\bar{y}) = F(G(\bar{y}))$ has gradient

$$(23)\quad F_y(\bar{y}) = G_y(\bar{y})\, F_z(\bar{z})$$

The method of differentiating equality constraints (task definition constraints) for inclusion in the penalty function will be indicated by an example. Suppose it is specified that a terminal point P_{I_m} is to reach control point C (a vector in C_o - coordinates).

As in section 3.3.2, this terminal constraint may be written

(24) $P_{I_m}(z) - C = 0.$

Define the equality-constraint vector to be $g(z) = P_{I_m}(z) - C$, a vector with three components. Using the transformation G which removes inequality constraints, we obtain the gradient matrix for the vector function $\hat{g}$ on y-space defined by $\hat{g}(y) = g(G(y))$:

(25) $\hat{g}_y(\bar{y}) = G_y(\bar{y})\, g_z(G(\bar{y}))$; $g_z(\bar{z})$ has the vector

$$\left(\frac{\partial P_{I_m}}{\partial z_K}\right)_{z=\bar{z}}$$ as its K-th row.

To summarize, the solution to the stick-man task-motion problem, as outlined in this section, is to optimize on the equality-inequality system:

(26)
minimize
$$F(z) = f(B(z)) + h(z)$$
subject to
$$g(z) = 0$$
and
$$\lambda_{z_i} \leq z_i \leq \mu_{z_i}$$
or
$$\lambda_{z_i}(z_{i+1}) \leq z_i \leq \mu_{z_i}(z_{i+1}).$$

Using the constraint - removal transformation G, we may choose to solve the equivalent problem

$$(27)\quad \begin{cases} \text{minimize} \\ \quad \hat{F}(y) = f(B(G(y))) + h(G(y)) \\ \text{subject to} \\ \quad g(G(y)) = 0, \end{cases}$$

where $G(y)$ is given by equations (17)' and (18)'. At present, the Davidon variable - metric method with penalty function is being tested as a gradient-projection method for solving the stick-man problem as formulated in (27).

PHASE I OBJECTIVE FUNCTION

So far, the objective function F that has been tried with this model is based in part on the simplifying notion that gravito - inertial effects can be ignored in formulating human motion criteria. This assumption means that the term $f(B(z))$ is missing from $F(z)$. Thus, F required no evaluation of the position coordinates $P_{I_i}(z)$ that make up the vector $x = B(z)$. These coordinates are needed only for the constraint vector $g(z)$.

The underlying assumption for the Phase I objective function F is that a human body prefers to stay as close as possible to fetal (or a "Dead Man Floating") position at all times. Thus, if values $z_i (i = 1,\ldots,n)$ are selected to be the fetal-position Euler angles, the squared deviations $(\Delta z_i)^2 = (z_i - z_i^o)^2$ of the angles from fetal position values are minimized. Originally, the form of $F(z)$ was

$$(28)\quad F(z) = \sum_{i=1}^{n} w_i (z - z_i^o)^2,$$

where the w_i are preassigned constants > 0 that express, for each i, the relative importance of keeping $(\Delta z_i)^2$ as small as possible. For example, the weight w_i for a deviation Δz_i in one of the spine-system (such as C_1) angles would be considerably

greater than the weight w_i for a deviation Δz_i in an angle that moves the radial link of one of the arms, since the entire upper torso certainly has a greater tendency to minimize muscular interference than a radial link.

The objective function in (28) was used with success on the one-arm model and provided a basis for further developmental work on the fetal position idea. Recently, another formulation has been tried with greater success. Let A be the set of Euler angles used in making up z, excluding the angles ϕ_{I_i} that appear as variables in some joints, i.e., joints where the direction of bend of link I_i is variable.

The new objective function is as follows: If z_i corresponds to a "twist" angle ψ_{I_i} or a "bend" angle θ_{I_i} for which ϕ_{I_i} is fixed, then form the term

(29) $F_K = w_K(z_K - z_K^o)^2$. If z_K is an angle θ_{I_i} for which ϕ_{I_i} varies, form the expression F_{K+1} for z_{K+1} as in (29), and for z_K form the term

(30) $F_K = w_K F_{K+1} (z_K - z_K^o)^2$.

The objective function is then formed as the sum

(31) $F(z) = \sum_{i \in A} F_i$. Here an attempt has been made to express the possible dependence of F_K on F_{K+1} when z_{K+1} is a variable "bend-direction" angle ϕ_{I_i}, instead of letting z_{K+1} affect F(z) independently.

It may be that the angles ϕ_{I_i} should be removed from consideration altogether in formulating an objective function such as (28) or (31); there may be no preferred direction-of-bend ϕ_{I_i} for a fetal position. Recent results obtained by setting $w_K = 0$ for $K \notin A$ (z_K is an angle ϕ_{I_i}) indicate that this is so.

Also, a better way of expressing the preferred orientations of some body segments, such as the lumbar region, may be needed. For example, it may be that the lumbar link has more than one preferred position in this formulation; e.g., if it is necessary for the simulated man to move his torso forward, a re-defined preferred Euler angle should be used to allow him to settle more readily into a "hunched-over" position. Results with movements requiring torso excursion strongly indicate this.

In conclusion, further work on the objective function formulation should include:

(1) continued research on improvements in the present idea,
(2) research on the validity of the simplifying assumptions made in ignoring the effects of gravity and body-segment momentum on the problem system, and
(3) reformulation of and developmental work on the objective function F as a result of such research.

The research on objective function formulation outlined above is in addition to that needed in other areas of analysis, such as improvements to the optimization method being used and investigation of the possibility of introducing time-dependence directly into the problem formulation by the use of additional transformations.

3.4 INTERFERENCE ANALYSIS

When a task is complete, it is necessary to determine whether BOEMAN-I was able to see the control for which he reached and whether his joint-link system, during the path of motion, encountered the work station geometry. Interference is the general term describing these situations. The first case is concerned with visual interference due to the intersection of BOEMAN's line of sight with one of the cockpit planes and the second case with physical interference due to the intersection of at least one link with these planes during the task.

The procedures of this section give the work station designer an indication of visual accessibility of controls as well as the dimensional fitness (to a given pilot's anthropometric characteristics) of the overall design during a task sequence.

When visual interference has occurred, it is desirable to attempt a modification of BOEMAN's point of view to regain visual contact with the control. The use of a corrected line of sight is an indicator of the visual complexity of the work station. Ideally, in any work station, visual interference due to the environment should not occur. In practice, environmental interference is to be minimized.

The rest of this section is concerned with detection of visual interference, the correction for this interference and the detection of physical interference (restricted to BOEMAN-I and the seat back planes). Correction of physical interference is not attempted during Phase I of the project.

NOTATION

$\hat{D}$ = Minimum distance from intersection point to a plane edge

$S_i, i=1,2$ = Coefficients of Centroid - intersection point line and plane edge, respectively

t_i, $i = 1,2,3$ = line and plane coefficients

V_j = (x_j,y_j,z_j) = j^{th} vertex of a cockpit plane

X = (x,y,z) = a point on the line of sight

X' = a point on redefined line of sight

$\hat{X}$ = intersection of Centroid - intersection point line with an edge of the cockpit plane

X_A = (x_5,y_5,z_5) = eye aiming point

X_C = (x_c,y_c,z_c) = Centroid of a plane P

X_M = (x_4,y_4,z_4) = Midpoint between the eyes

X_{MP} = $\frac{1}{2}(X_M + X_A)$ = (x_6,y_6,z_6) = Midpoint of line of sight

Y = nearest point to original intersection point in the plane

3.4.1 Visual Interference

For the baseline model, the Cockpit Geometry is assumed to be composed of bounded planes which are polygons with four, five or six sides. These planes describe the panels and solid surfaces of the work station.

A line of sight is defined with the end points given by the eye midpoint and the task defined control point, on which the eye is to "focus".

It is required to determine if any of the bounded planes intersect with the line of sight and if so, whether it is possible to define a new line of sight, by moving BOEMAN's eye midpoint, for which no intersection with the offending plane will occur.

These problems are the detection of, and the correction for, visual interference.

DETECTION OF VISUAL INTERFERENCE

It is necessary to determine if the line of sight bounded by the eye midpoint, calculated by the motion model and the eye aiming point specified by the task, intersects any cockpit plane.

Let $X_M = (x_4, y_4, z_4)$ = the midpoint between the eyes.
$X_A = (x_5, y_5, z_5)$ = the eye aiming point
$X = (x, y, z)$ = a point on the line of sight

Then the equation of the line between these points is given by

$$X = (1 - t_3)\, X_M + t_3\, X_A$$

or

$$(1)\quad \begin{cases} x = (1-t_3)\,x_4 + t_3\,x_5 \\ y = (1-t_3)\,y_4 + t_3\,y_5 \\ z = (1-t_3)\,z_4 + t_3\,z_5 \end{cases}$$

where $0 \leq t_3 < 1$

Because it is not possible to easily describe a bounded plane with four or more vertices in analogous form as (1), the following procedure is used.

Let V_j be the vertices of any plane in the cockpit.

The V_j are ordered such that V_j is adjacent to V_{j+1}.

Let V_1, V_2, V_3 be representative of the plane P with

$V_j = (x_j, y_j, z_j)$ for $j = 1, 2, 3$. (See Figure 16)

Then the equation of an infinite plane* in which P is embedded, is given by

$$X = t_1V_1 + t_2V_2 + (1-t_1-t_2)V_3$$

or

$$(2)\quad \begin{cases} x = t_1x_1 + t_2x_2 + (1-t_1-t_2)\,x_3 \\ y = t_1y_1 + t_2y_2 + (1-t_1-t_2)\,y_3 \\ z = t_1z_1 + t_2z_2 + (1-t_1-t_2)\,z_3 \end{cases}$$

with no restriction on t_1 and t_2

The line of sight and the infinite plane are tested for an intersection point. If there are none, the line is parallel to the infinite plane; If there are two or more, the line is embedded within the plane. Otherwise a single unique solution exists to (1), (2).

---

*Olmsted, John, M. H., Solid Analytic Geometry, Appleton-Century Crofts, Chapter 2.

Thus, setting (1) and (2) equal to each other and rearranging yields

$$(V_1 - V_3)\, t_1 + (V_2 - V_3)\, t_2 + (X_M - X_A)\, t_3 = X_M - V_3$$

$$(3)\quad \begin{cases} (x_1 - x_3)\, t_1 + (x_2 - x_3)\, t_2 + (x_4 - x_5)\, t_3 = x_4 - x_3 \\ (y_1 - y_3)\, t_1 + (y_2 - y_3)\, t_2 + (y_4 - y_5)\, t_3 = y_4 - y_3 \\ (z_1 - z_3)\, t_1 + (z_2 - z_3)\, t_2 + (z_4 - z_5)\, t_3 = z_4 - z_3 \end{cases}$$

Solving by determinants, let

$$(4)\quad D = \begin{vmatrix} (x_1 - x_3) & (x_2 - x_3) & (x_4 - x_5) \\ (y_1 - y_3) & (y_2 - y_3) & (y_4 - y_5) \\ (z_1 - z_3) & (z_2 - z_3) & (z_4 - z_5) \end{vmatrix}$$

$$(5)\quad A = \begin{vmatrix} (x_4 - x_3) & (x_2 - x_3) & (x_4 - x_5) \\ (y_4 - y_3) & (y_2 - y_3) & (y_4 - y_5) \\ (z_4 - z_3) & (z_2 - z_3) & (z_4 - z_5) \end{vmatrix}$$

$$(6)\quad B = \begin{vmatrix} (x_1 - x_3) & (x_4 - x_3) & (x_4 - x_5) \\ (y_1 - y_3) & (y_4 - y_3) & (y_4 - y_5) \\ (z_1 - z_3) & (z_4 - z_3) & (z_4 - z_5) \end{vmatrix}$$

$$(7)\quad C = \begin{vmatrix} (x_1 - x_3) & (x_2 - x_3) & (x_4 - x_3) \\ (y_1 - y_3) & (y_2 - y_3) & (y_4 - y_3) \\ (z_1 - z_3) & (z_2 - z_3) & (z_4 - z_3) \end{vmatrix}$$

whence

$$(8)\qquad \left.\begin{aligned} t_1 &= \frac{A}{D} \\ t_2 &= \frac{B}{D} \\ t_3 &= \frac{C}{D} \end{aligned}\right\} \qquad \text{(provided that } D \neq 0\text{)}$$

If D = 0, then either no solution or many solutions exist. To distinguish between these cases, the midpoint of the line of sight is substituted into the equation of a plane (in determinant form). If it is satisfied, the entire line must be embedded. If it is not satisfied, the line is parallel to the plane.

Thus

$$(9)\qquad \mathbf{X}_{MP} = \tfrac{1}{2}\mathbf{X}_{M} + \tfrac{1}{2}\mathbf{X}_{A}\ ,\ \mathbf{X}_{MP} = (x_6, y_6, z_6)$$

is the midpoint of the line of sight.

A theorem in solid analytic geometry states*: "A necessary and sufficient condition for four points to be co-planar (x_i, y_i, z_i), i = 1,2,3,4, is that the determinant

$$\begin{vmatrix} x_4 & y_4 & z_4 & 1 \\ x_1 & y_1 & z_1 & 1 \\ x_2 & y_2 & z_2 & 1 \\ x_3 & y_3 & z_3 & 1 \end{vmatrix} = 0."$$

* Olmsted, John M. N., Solid Analytic Geometry, Appleton-Century-Crofts, p. 74.

In this case

$$(10)\quad \begin{vmatrix} x_6 & y_6 & z_6 & 1 \\ x_1 & y_1 & z_1 & 1 \\ x_2 & y_2 & z_2 & 1 \\ x_3 & y_3 & z_3 & 1 \end{vmatrix} = 0$$

If (10) is not satisfied, the line is parallel to the plane, and there is no visual interference. It is expected that a line embedded in a plane would not ordinarily occur. If it did, an infinitesimal movement of the eye midpoint would eliminate the interference, so that this case need not be considered in further detail.

Suppose then, that $D \neq 0$. If interference is to occur, it is necessary that t_3 in (8) satisfy

$$0 \leq t_3 < 1 \quad \text{as in (1).}$$

($t_3 = 1$ implies that the intersection of the line of sight and the cockpit plane occurs at the eye aiming point which is a normal occurrence.) If not, there is no interference.

If so, one must determine if the intersection has occurred within the bounded plane or outside it. For this the centroid, X_c, of the plane is calculated using the vertices V_j of the plane

$$X_c = (x_c, y_c, z_c) \text{ and}$$

$$(11) \quad X_c = \frac{\sum_{j=1}^{n} V_j}{n}$$

or

$$x_c = \frac{\sum_{j=1}^{n} x_j}{n}, \quad y_c = \frac{\sum_{j=1}^{n} y_j}{n}, \quad z_c = \frac{\sum_{j=1}^{n} z_j}{n}$$

To determine if the intersection point is within the bounded plane, a line is drawn from the intersection point $\hat{X}$ to the centroid of the plane X_c, known to be inside the bounded plane. If this line segment crosses any one of the edges of the plane (V_j, V_{j+1}) then $\hat{X}$ is outside the bounded plane.

If none of the edges are crossed, $\hat{X}$ must be within the bounded plane.

Thus we have

(12) Centroid Intersection Line

$$\hat{X} = X \cdot S_1 + X_c \cdot (1-S_1), \quad 0 \leq S_1 \leq 1$$

where $\hat{X}$ is a point on this line

(13) Plane Edge

$$\hat{X} = V_j \cdot S_2 + V_{j+1} \cdot (1-S_2) \qquad 0 \leq S_2 \leq 1$$

$$j = 1, \ldots, n;$$

$$V_{n+1} = V_1$$

where $\hat{X}$ is a point on an edge of a plane.

If no common solution $\hat{X}$ of (12) and (13) exists for any j, then $\hat{X}$ is within the bounded plane and interference exists. Otherwise, there is no interference. Figures 16 and 17 describe each situation. Thus in all cases, one may detect the occurrence of visual interference.

CORRECTION FOR VISUAL INTERFERENCE .

It is necessary to distinguish between two kinds of correction techniques: The general and the specific. The general technique provides a method of relocating the line of sight given any work station configuration and under any circumstances. A specific method, described below, is geared towards a simple cockpit geometry in which the occurrences of interference during a task sequence will be rare. Under this assumption, the situation where a single plane causes interference is examined. Visually complex cockpits, where two or more planes simultaneously cause interference, require the more general method for solution and are beyond the scope of the Baseline Man-Model for Phase I.

An analysis of the multimission simulator shows that the resulting planes are connected to each other at their boundaries and that sources of interference occur only for the collection of planes forming the "head-up display" and the control stick platform surfaces. In each case, interference would occur with only the top or front planes of the surface. Thus, it is sufficient to examine a corrective measure for interference with a single plane.

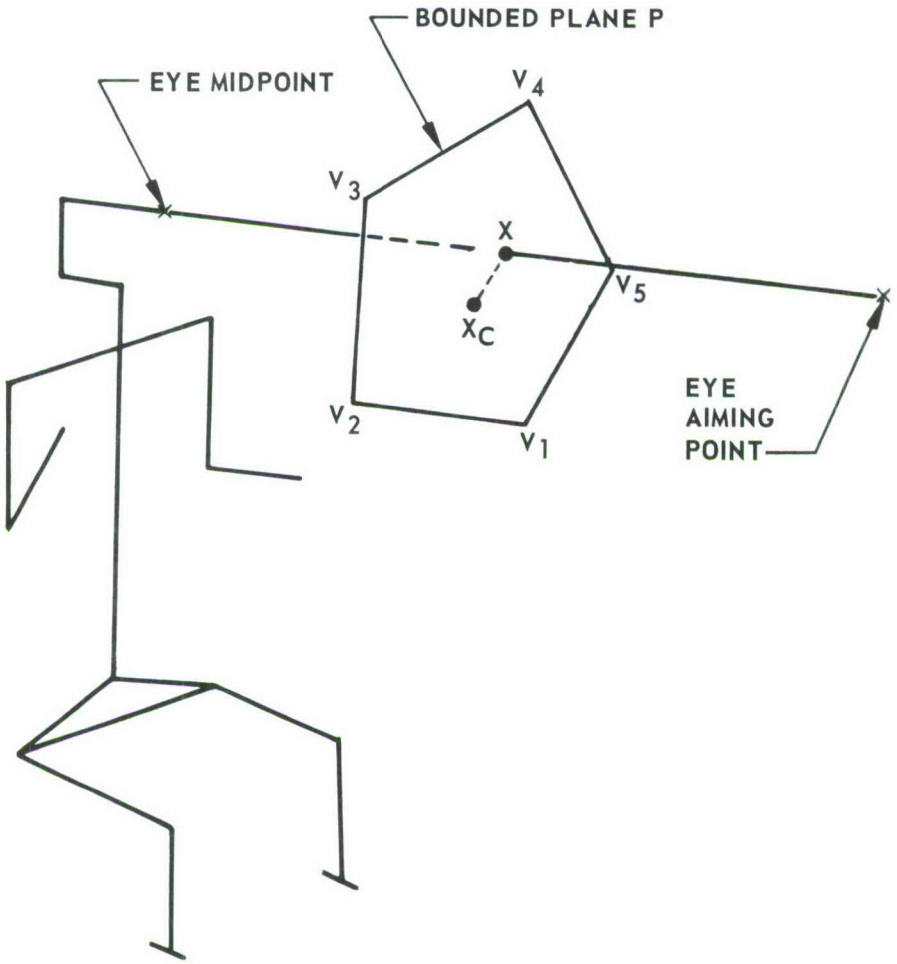

Figure 16. Occurrence of Visual Interference

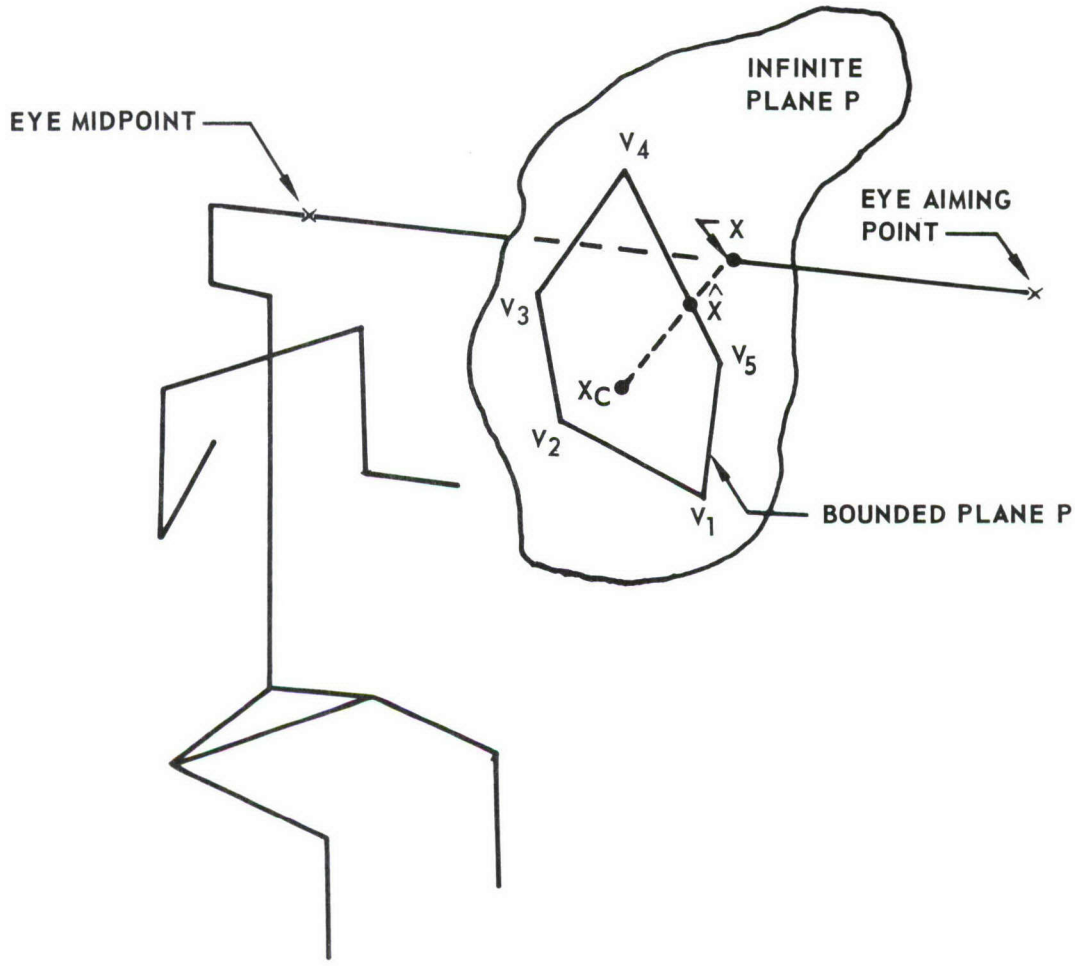

Figure 17. Visual Interference-Free Situation

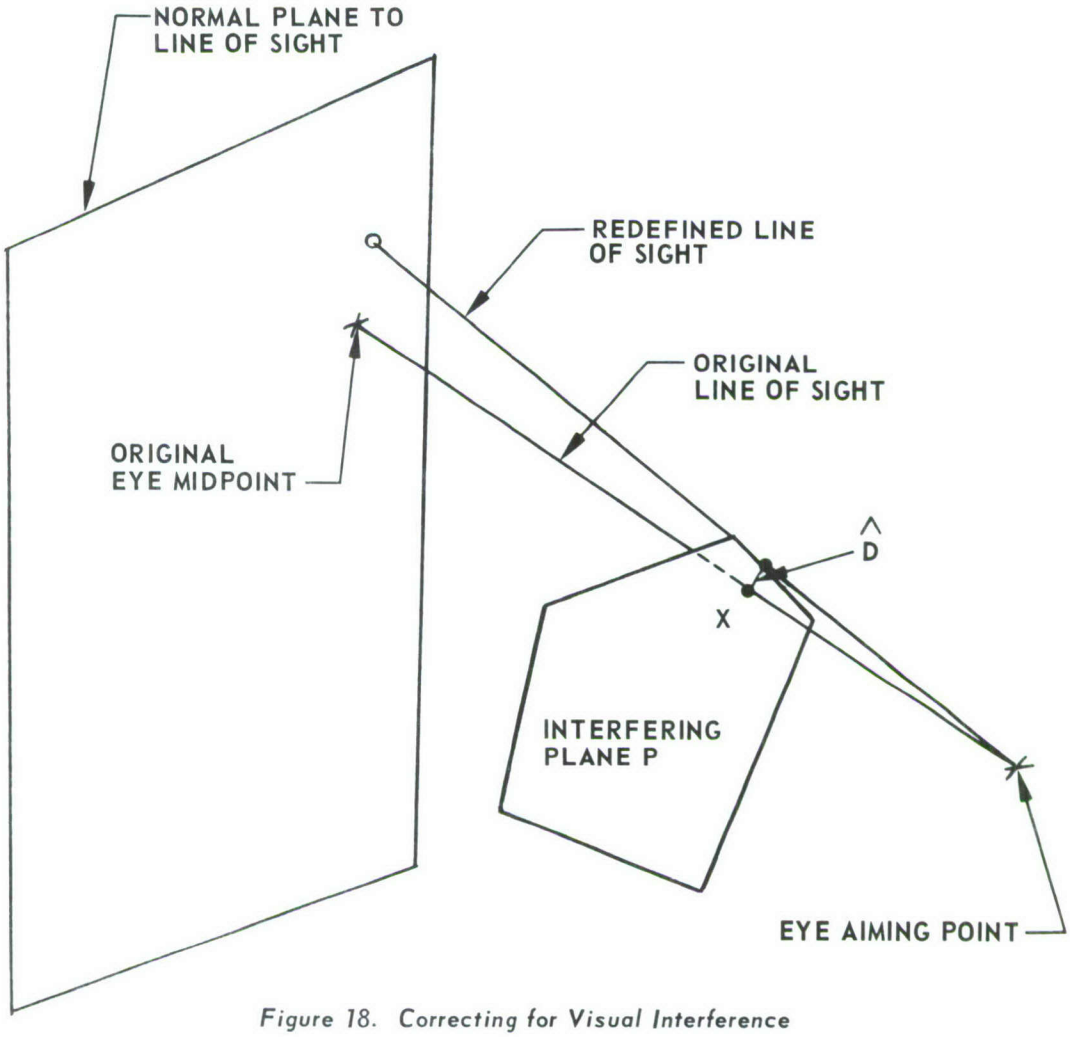

Figure 18. Correcting for Visual Interference

If the line of sight is to be deflected, it is desired that it be moved to a point on the edge of the plane whose distance from the point of intersection is a minimum. This situation is described in Figure 18.

To accomplish this it is necessary to find a line perpendicular to an edge of the plane with one end point at the intersection point X such that its distance D is the minimum of all possible perpendicular lines to every side of the plane.

Consider a plane P with intersection point X as in figure 19.

Let P have vertices V_j $(j = 1,2,\ldots,7)$ with $V_7 = V_1$.

In particular, let

$$(14)\quad d_{1_j} = V_{j+1} - V_j = + \left((x_{j+1}-x_j)^2 + (y_{j+1}-y)^2 + (z_{j+1}-z_j)^2 \right)^{1/2}$$

$$(15)\quad d_{2_j} = V_{j+1} - X = + \left((x_{j+1}-x_I)^2 + (y_{j+1}-y_I)^2 + (z_{j+1}-z_I)^2 \right)^{1/2}$$

$$(16)\quad d_{3_j} = + \sqrt{d_{2_j}^2 - D_j^2}$$

where I denotes the intersection point on the plane and D_j is defined by

$$(17)\quad D_j = d_{2_j} \sin \alpha \ .$$

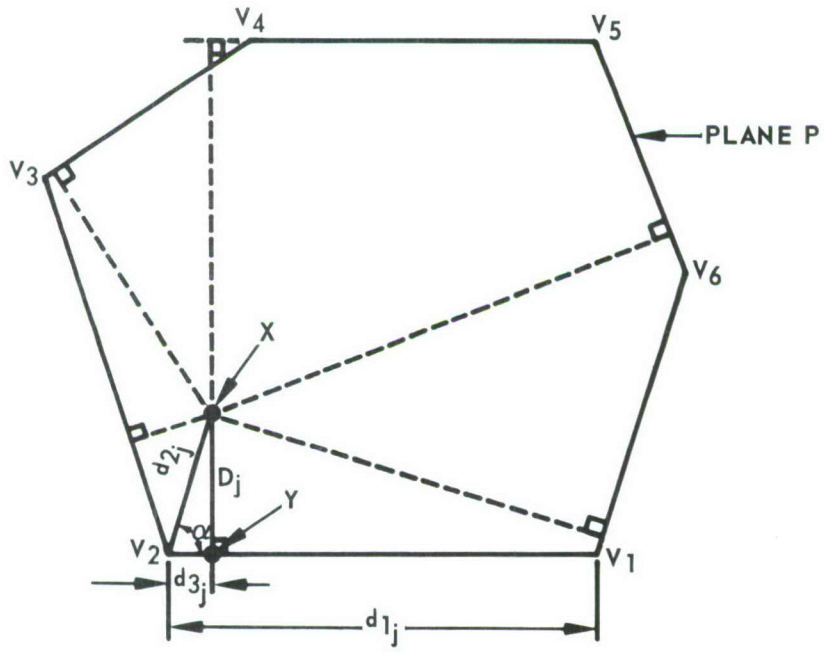

Figure 19. Determination of Minimum Distance to Edge of Bounded Plane

Since α is not available directly, another theorem of solid analytic geometry is invoked,* stating "if α is the angle between two directions $(\lambda_1, \mu_1, \nu_1)$ and $(\lambda_2, \mu_2, \nu_2)$ then

$$\sin^2\alpha = \begin{vmatrix} \mu_1 & \nu_1 \\ \mu_2 & \nu_2 \end{vmatrix}^2 + \begin{vmatrix} \nu_1 & \lambda_1 \\ \nu_2 & \lambda_2 \end{vmatrix}^2 + \begin{vmatrix} \lambda_1 & \mu_1 \\ \lambda_2 & \mu_2 \end{vmatrix}^2 \quad "$$

Let

$$\lambda_{2_j} = (x_{j+1}-x_j)/d_{1_j} \qquad \lambda_{1_j} = (x_I-x_{j+1})/d_{2_j}$$

$$\mu_{2_j} = (y_{j+1}-y_j)/d_{1_j} \qquad \mu_{1_j} = (y_I-y_{j+1})/d_{2_j}$$

$$\nu_{2_j} = (z_{j+1}-z_j)/d_{1_j} \qquad \nu_{1_j} = (z_I-z_{j+1})/d_{2_j}$$

Then using (17) directly,

$$(18)\quad D_j = + \left(\begin{vmatrix} (y_I-y_{j+1}) & (z_I-z_{j+1}) \\ \mu_{2_j} & \nu_{2_j} \end{vmatrix}^2 + \begin{vmatrix} (z_I-z_{j+1}) & (x_I-x_{j+1}) \\ \nu_{2_j} & \lambda_{2_j} \end{vmatrix}^2 + \begin{vmatrix} (x_I-x_{j+1}) & (y_I-y_{j+1}) \\ \lambda_{2_j} & \mu_{2_j} \end{vmatrix}^2 \right)^{1/2}$$

then choosing the minimum $\hat{D} = \underset{j}{\text{Min}}\,(D_j)$

The location of the nearest point Y on the closest edge of the plane may be described as follows:

$$(19)\quad \text{let}\quad u_1 = \frac{\hat{d}_3}{\hat{d}_1}$$

* Op. Cit. , P. 21

Then Y can be given by

(20) $Y = u_1 V_j + (1 - u_1) V_{j+1}$

Finally, the redefined line of sight is given in terms of Y and the eye aiming point, X_A as

(21) $X' = t' Y + (1-t') X_A; \quad t' > 1$

where X' is any point on the redefined line of sight in front of the interfering plane (towards BOEMAN-I).

3.4.2 Physical Interference

Since BOEMAN-I moves in a rigid environment it is desirable to have an indication of when link intersections occur with the surrounding geometry.

For Phase I, attention is restricted to the most probable planar encounter - the seat back. In general, hand positions are given and presumed consistent with the geometric configuration (no intersection). However, intersection with the seat back is possible for all interior joints and links.

Future phases will be more concerned with the general detection and correction of physical interference.

DETECTION OF PHYSICAL INTERFERENCE

The problem of detection is handled similarly to that in Section 3.4.1. The line of sight corresponds to a link (line between two joints) and the seat back plane corresponds to the cockpit planes.

Each of the links are tested in turn during each step in the task and all seat back interference is determined.

Let (X_k, X_{k+1}) be the k^{th} link between points X_k, X_{k+1} let V_j denote the vertices of the seat back, then

(22) $X(k) = t_3 X_k + (1-t_3)X_{k+1}$ $\quad 0 \leq t_3 \leq 1$, $k = 1,\ldots, m$

is the equation of the link line, where m is the total number of links under consideration and

(23) $X = t_1 V_1 + t_2 V_2 + (1-t_1-t_2)V_3$ (where t_1 and t_2 are suitable constants) is the equation for the seat back with vertices V_1, V_2, V_3.

Setting (22) and (23) equal yields

(24) $(V_1-V_3)t_1 + (V_2-V_3)t_2 + (X_k-X_{k+1})t_3 = X_{k+1}-V_3$

Using determinants to solve for t_1, t_2, and t_3 similar formulas as in (4) - (18) are generated. Then, if $0 < t_3 < 1$ is not true, physical interference has not occurred. ($t_3 = 0$ or 1 imply only that a joint is coincident with the seat back.

Using (11) to calculate the seat back centroid X_c, the centroid intersection line is generated, along with the seat back plane edge:

(25) $\bar{X} = XS_1 + X_c (1-S_1)$ $\quad 0 \leq S_1 \leq 1$; $k=1,\ldots, m$

(26) $\bar{X} = V_j S_2 + V_{j+1}(1-S_2)$ $\quad 0 \leq S_2 \leq 1$ $j=1,\ldots, n$ and $V_{n+1}=V_1$

where m is the number of links under consideration and $\bar{X}$ represents a common point on both lines. If no common solution $\bar{X}$ exists for any j, then X is within the seat back plane and physical interference has occurred.

Each link is tested in this fashion and the resulting physical interference is indicated.

In contrast to the visual interference section, no correction for physical interference is attempted in Phase I since a correction procedure would actively involve the optimization model. An overall procedure for determining and correcting interference during the motion is scheduled, for Phase II.

4.0 REFERENCES

1. Davidon, W. C., Variable Metric Method for Minimization, Argonne National Lab Report ANL-5990 R, November 1959.

2. Fletcher, R., and Powell, M. J. D., "A Rapidly Convergent Descent Method for Minimization", Computer Journal 6, pp 163-168, 1963.

3. Johnson, I. L., Jr., and Myers, G. E., One-Dimensional Minimization Using Search By Golden Section and Cubic Fit Methods, NASA Report, Mission Planning and Analysis Division, Manned Spacecraft Center, November 13, 1967.

4. Kelley, H. J., Denham, W. F., Johnson, I. L., and Wheatley, P. O., "An Accelerated Gradient Method For Parameter Optimization With Non-Linear Constraints", The Journal of the Astronautical Sciences, Vol. XIII, No. 4, pp 166-169, July - August, 1966.

5. Kowalik, J., Nonlinear Programming Procedures and Design Optimization, Acta Polytechnical Scandinavica, Trondheim, 1966.

6. Olmsted, J. M. H., Solid Analytic Geometry, Appleton - Century-Crofts.

7. Gagnon, K., Fortran IV Subroutine MINUM, Coordination Sheet No. MA-077, Boeing Company, November 23, 1966 (Appendix IX of D162-10127-1)

ACTIVE SHEET RECORD

SHEET NUMBER	REV LTR	ADDED SHEETS				SHEET NUMBER	REV LTR	ADDED SHEETS			
		SHEET NUMBER	REV LTR	SHEET NUMBER	REV LTR			SHEET NUMBER	REV LTR	SHEET NUMBER	REV LTR
1-93											

DISTRIBUTION LIST

Office of Naval Research
Aeronautics, Code 461
Department of the Navy
Washington, D. C. 20360
ATTN: LCDR F. L. Cundari (2)

Commanding Officer
U. S. Naval Missile Center
Box 15
Point Mugu, California 93041
ATTN: Code 5342 (1)

Commanding Officer
U. S. Army Human Engineering Labs.
Aberdeen Proving Grounds
Aberdeen, Maryland 21005
ATTN: AMXHE-SYS (J. Barnes) (1)

U. S. Army Natick Laboratories
Anthropology Group
Pioneering Research Lab.
Natick, Massachusetts 01760
ATTN: R. M. White (5)

Defense Documentation Center
Cameron Station
Alexandria, Virginia 22314 (2)

Commander
U. S. Army Aeromedical Research Lab.
Fort Rucker, Alabama 36360
ATTN: LTCOL D. E. Littell (1)

Commander
Naval Air Systems Command
Washington, D. C. 20360
ATTN: NAVAIR 53371 (1)
NAVAIR 5313 (2)

Commander
U. S. Naval Air Development Center
Johnsville, Warminster, Pa. 18974
ATTN: AMXI-V (1)
ACEL (5)

Commander
U. S. Naval Test Center
Aeromedical Branch
Service Test Division
Patuxent River, Maryland 20670 (1)

Director
U. S. Naval Research Laboratory
Washington, D. C. 20390
ATTN: Tech Info Office (1)

Commanding General
U. S. Army Electronics Command
Fort Monmouth, New Jersey 07703
ATTN: AMSEL-VL-I (3)

Commander
USAF 6570th Aero Medical Research Laboratory
Wright-Patterson AFB
Dayton, Ohio 45433
ATTN: AMRL (MRHA) (5)

DOCUMENT CONTROL DATA - R & D

(Security classification of title, body of abstract and indexing annotation must be entered when the overall report is classified)

1. ORIGINATING ACTIVITY (Corporate author)
The Boeing Company
P. O. Box 3955
Seattle, Washington 98124

2a. REPORT SECURITY CLASSIFICATION
Unclassified

2b. GROUP
N/A

3. REPORT TITLE
COCKPIT GEOMETRY EVALUATION - PHASE I FINAL REPORT
VOLUME IV: MATHEMATICAL MODEL

4. DESCRIPTIVE NOTES (Type of report and inclusive dates)
Phase I Final Report, 15 January 1968 - 31 December 1968

5. AUTHOR(S) (First name, middle initial, last name)
Healy, Michael J.
Katz, Robert (NMI)

6. REPORT DATE
January 1969

7a. TOTAL NO. OF PAGES
93

7b. NO. OF REFS
7

8a. CONTRACT OR GRANT NO.
N00014-68-C-0289

b. PROJECT NO.
NR 213-065

c.

d.

9a. ORIGINATOR'S REPORT NUMBER(S)
D162-10128-1

9b. OTHER REPORT NO(S) (Any other numbers that may be assigned this report)
JANAIR REPORT 690104

10. DISTRIBUTION STATEMENT
This document has been approved for public release and sale; its distribution is unlimited.

11. SUPPLEMENTARY NOTES
N/A

12. SPONSORING MILITARY ACTIVITY
Office of Naval Research
Department of the Navy
Aeronautics, Code 461
Washington, D. C. 20360

13. ABSTRACT

A mathematical model that positions and moves a variable sized 23-pin joint articulated stick-man in a crewstation environment is presented. The model simulates the motion of pilots in a given cockpit configuration considering gross reach capability required by a task. It utilizes a non-linear optimization technique to position and orient the joints, analyzes the viewing capability after the operation and detects body intersections with the seatback during the task. (U)

The distribution of this abstract is unlimited

DD FORM 1 NOV 65 1473

14 KEY WORDS		LINK A		LINK B		LINK C	
		ROLE	WT.	ROLE	WT.	ROLE	WT.
Cockpit	Non-Linear						
Design	Optimization						
Geometry	Performance						
Human	Simulation						
Man-Model							
Minimization							

INSTRUCTIONS

1. ORIGINATING ACTIVITY: Enter the name and address of the contractor, subcontractor, grantee, Department of Defense activity or other organization *(corporate author)* issuing the report.

2*a*. REPORT SECURITY CLASSIFICATION: Enter the overall security classification of the report. Indicate whether "Restricted Data" is included. Marking is to be in accordance with appropriate security regulations.

2*b*. GROUP: Automatic downgrading is specified in DoD Directive 5200.10 and Armed Forces Industrial Manual. Enter the group number. Also, when applicable, show that optional markings have been used for Group 3 and Group 4 as authorized.

3. REPORT TITLE: Enter the complete report title in all capital letters. Titles in all cases should be unclassified. If a meaningful title cannot be selected without classification, show title classification in all capitals in parenthesis immediately following the title.

4. DESCRIPTIVE NOTES: If appropriate, enter the type of report, e.g., interim, progress, summary, annual, or final. Give the inclusive dates when a specific reporting period is covered.

5. AUTHOR(S): Enter the name(s) of author(s) as shown on or in the report. Enter last name, first name, middle initial. If military, show rank and branch of service. The name of the principal author is an absolute minimum requirement.

6. REPORT DATE: Enter the date of the report as day, month, year; or month, year. If more than one date appears on the report, use date of publication.

7*a*. TOTAL NUMBER OF PAGES: The total page count should follow normal pagination procedures, i.e., enter the number of pages containing information.

7*b*. NUMBER OF REFERENCES: Enter the total number of references cited in the report.

8*a*. CONTRACT OR GRANT NUMBER: If appropriate, enter the applicable number of the contract or grant under which the report was written.

8*b*, 8*c*, & 8*d*. PROJECT NUMBER: Enter the appropriate military department identification, such as project number, subproject number, system numbers, task number, etc.

9*a*. ORIGINATOR'S REPORT NUMBER(S): Enter the official report number by which the document will be identified and controlled by the originating activity. This number must be unique to this report.

9*b*. OTHER REPORT NUMBER(S): If the report has been assigned any other report numbers *(either by the originator or by the sponsor)*, also enter this number(s).

10. AVAILABILITY/LIMITATION NOTICES: Enter any limitations on further dissemination of the report, other than those imposed by security classification, using standard statements such as:

(1) "Qualified requesters may obtain copies of this report from DDC."

(2) "Foreign announcement and dissemination of this report by DDC is not authorized."

(3) "U. S. Government agencies may obtain copies of this report directly from DDC. Other qualified DDC users shall request through _____."

(4) "U. S. military agencies may obtain copies of this report directly from DDC. Other qualified users shall request through _____."

(5) "All distribution of this report is controlled. Qualified DDC users shall request through _____."

If the report has been furnished to the Office of Technical Services, Department of Commerce, for sale to the public, indicate this fact and enter the price, if known.

11. SUPPLEMENTARY NOTES: Use for additional explanatory notes.

12. SPONSORING MILITARY ACTIVITY: Enter the name of the departmental project office or laboratory sponsoring *(paying for)* the research and development. Include address.

13. ABSTRACT: Enter an abstract giving a brief and factual summary of the document indicative of the report, even though it may also appear elsewhere in the body of the technical report. If additional space is required, a continuation sheet shall be attached.

It is highly desirable that the abstract of classified reports be unclassified. Each paragraph of the abstract shall end with an indication of the military security classification of the information in the paragraph, represented as *(TS), (S), (C), or (U)*.

There is no limitation on the length of the abstract. However, the suggested length is from 150 to 225 words.

14. KEY WORDS: Key words are technically meaningful terms or short phrases that characterize a report and may be used as index entries for cataloging the report. Key words must be selected so that no security classification is required. Identifiers, such as equipment model designation, trade name, military project code name, geographic location, may be used as key words but will be followed by an indication of technical context. The assignment of links, rules, and weights is optional.

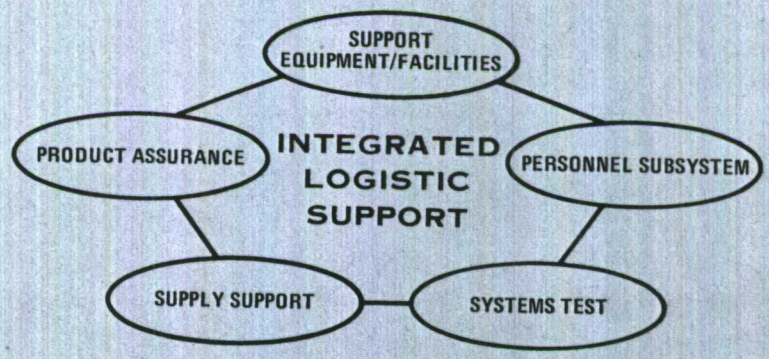
SUPPORT EQUIPMENT/FACILITIES
PRODUCT ASSURANCE
INTEGRATED LOGISTIC SUPPORT
PERSONNEL SUBSYSTEM
SUPPLY SUPPORT
SYSTEMS TEST